

Contents lists available at ScienceDirect

Chemosphere

journal homepage: www.elsevier.com/locate/chemosphere





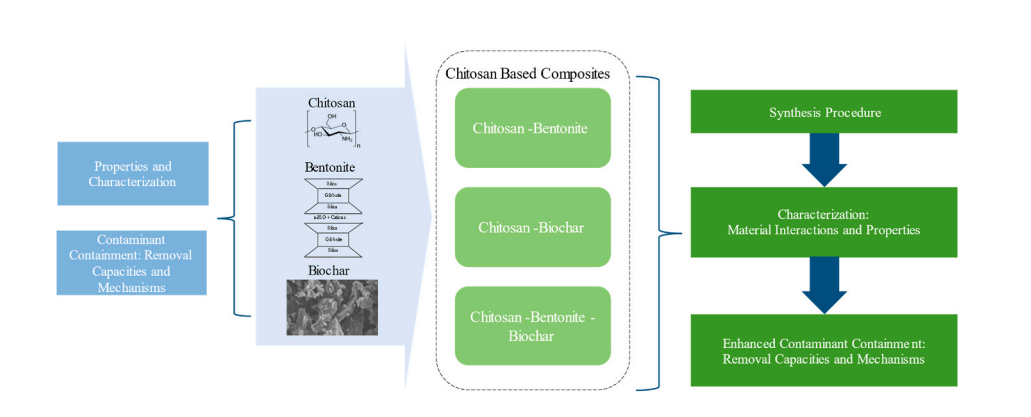
Novel chitosan-based barrier materials for environmental containment: Synthesis, characterization, and contaminant removal capacities and mechanisms

Banuchandra Nagaraja ^a, Jagadeesh Kumar Janga ^a, Sadam Hossain ^b, Gaurav Verma ^a, Angelica M. Palomino ^b, Krishna R. Reddy ^a, ^{*}

HIGHLIGHTS

- Chitosan with highly reactive functional groups is effective for contaminant removal.
- Bentonite is a desirable composite constituent for contaminant removal due to its surface area and anionic nature.
- Biochar in the composite increases surface area for contaminant adsorption.
- Composite synthesis procedures vary depending on the application.
- Contaminant removal by composites varied widely due to the variability in materials.

G R A P H I C A L A B S T R A C T



ARTICLE INFO

Handling Editor: Y Yeomin Yoon

Keywords:
Subsurface contamination
Containment barriers
Chitosan
Biochar
Bentonite
Adsorption
Composite barrier

ABSTRACT

This study critically appraises employing chitosan as a composite with bentonite, biochar, or both materials as an alternative to conventional barrier materials. A comprehensive literature review was conducted to identify the studies reporting chitosan-bentonite composite (CBC), chitosan amended biochar (CAB), and chitosan-bentonite-biochar composite (CBBC) for effective removal of various contaminants. The study aims to review the synthesis of these composites, identify fundamental properties affecting their adsorption capacities, and examine how these properties affect or enhance the removal abilities of other materials within the composite. Notably, CBC composites have the advantage of adsorbing both cationic and anionic species, such as heavy metals and dyes, due to the cationic nature of chitosan and the anionic nature of montmorillonite, along with the increased accessible surface area due to the clay. CAB composites have the unique advantage of being low-cost sorbents with high specific surface area, affinity for a wide range of contaminants owing to the high surface area and microporosity of biochar, and abundant available functional groups from the chitosan. Limited studies have reported the utilization of CBBC composites to remove various contaminants. These composites can be prepared by combining the steps employed in preparing CBC and CAB composites. They can benefit from the favorable

E-mail addresses: bn20@uic.edu (B. Nagaraja), jreddy3@uic.edu (J.K. Janga), mhossa39@vols.utk.edu (S. Hossain), gverma5@uic.edu (G. Verma), apalomin@utk.edu (A.M. Palomino), kreddy@uic.edu (K.R. Reddy).

a Department of Civil, Materials, and Environmental Engineering, University of Illinois Chicago, 842 West Taylor Street, Chicago, IL, 60607, USA

b Department of Civil and Environmental Engineering, University of Tennessee Knoxville, 423 John D. Tickle Building, Knoxville, TN, 37996, USA

^{*} Corresponding author.

adsorption properties of all three materials while also satisfying the mechanical requirements of a barrier material. This study serves as a knowledge base for future research to develop novel composite barrier materials by incorporating chitosan and biochar as amendments to bentonite.

1. Introduction

Climate change has been linked to various extreme events, such as flooding, sea level rise, and saltwater intrusion (Reddy et al., 2019; IPCC, 2021). Floods are one of the most common natural disasters in the US, affecting almost every state and county (NRDC, 2021). They pose not only an immediate threat to lives and properties but also present risks of exposure to contaminants which can have long-term effects (USGAO, 2021). Flood water often carries undesirable objects and harmful contaminants. Coastal flooding brings the risks of saltwater intrusion. At the same time, inland contaminated flood waters increase the risk of surface water bodies such as stormwater retention ponds and of groundwater contamination due to seepage from stormwater retention ponds and recharging the aquifers from surface water bodies.

One traditional approach to mitigating seepage of contaminated stormwater and containing groundwater contamination is the use of engineered barriers, such as low-permeability soil liners, placed at the base of stormwater retention ponds or vertical barriers (commonly known as slurry walls) constructed around the polluted groundwater in the subsurface. Low-permeability liners may include soil liners, admixed soil liners, or geosynthetic clay liners (GCLs). Slurry walls comprise backfill consisting of soil, bentonite, and water in excavated trenches as an engineered slurry for stability. The low permeability of the liners controls infiltration from retention ponds, while slurry wall backfill controls the passage of contaminated groundwater across the slurry wall.

In general, barrier materials, specifically for pond liners or backfills for the slurry walls, are selected based on the type of contaminants prevalent at the site and subsurface conditions (Rowe, 2001). However, the physicochemical properties of stormwater or groundwater, such as alkalinity, ionic strength, pH, temperature, dissolved oxygen, and dissolved organic matter, may be highly variable due to flooding events (Pitt et al., 1995). Hence, there is a need to develop effective barrier systems with sustainable and resilient materials that are compatible with a wide range of contaminants and adaptive to changing climatic conditions.

Developing novel materials for flood water containment and remediation requires a vast variety of contaminants to be considered. Thus, an engineered barrier material must be compatible with a wide range of key characteristics of contaminants, such as molecule size, binding mechanisms, and charge. Desired properties of engineered containment and remediation materials are chemical and thermal stability, microand mesoporous structure, large surface area, presence of many functional groups on the surface, and a high potential for regeneration. In addition, the materials should be economical, have low production costs, be scalable to address a wide range of conditions, and have high removal efficiencies (Aizat and Aziz, 2019; Wan Ngah et al., 2011).

In this regard, composites composed of alternative materials, such as chitosan and biochar, may fill the need for robust liner materials. The combined characteristics of chitosan, biochar, and bentonite may create a unique composite that will not only be able to control seepage but also retard or degrade a wide range of contaminant types, thereby protecting the physical and functional integrity of the barrier systems.

Chitosan is derived from chitin, the most abundant naturally occurring biopolymer after cellulose (Muzzarrelli, 1977). While there are many natural sources of chitin (e.g., sea animals, insects, fungi), the main source of chitin is crustacean shells (Rinaudo, 2006; Pal et al., 2021), which are often the waste products of the seafood industry and therefore available at low-cost. Crustacean shells comprise a significant portion of seafood processing waste, ~50–70% (Kumar et al., 2018), and

shrimp and crab processing wastes comprise 13–27% chitin by dry weight (Ashford et al., 1977). Chitosan is a widely available natural resource with abundant presence in nature and is less cost-intensive. It is cationic under slightly acidic conditions, biocompatible with human and animal tissue, biodegradable, non-toxic, and easily combined with other constituents to synthesize customized adsorption materials. Furthermore, chitosan has a high adsorption capacity and can readily adsorb contaminants ranging from low to high concentrations (Kumar, 2000; Synowiecki and Al-Khateeb, 2003; Sudha, 2010). Chitosan complexes have also been used for environmental remediation applications such as treating metal-laden waste streams (Robinson-Lora and Brennan, 2010). Chitosan serves as an electron donor, which may support biological processes or bioremediation of contaminants (Robinson-Lora and Brennan, 2009). Moreover, chitosan is available in particulate form, which makes it ideal for addition to liner and slurry wall backfill.

Biochar is a solid carbonaceous material produced from waste biomass through pyrolysis or gasification under oxygen-deficient conditions. Biochar is characterized by unique properties such as high moisture retention, high microporosity, and surface area, and high absorption potential for liquid and gaseous compounds (Yargicoglu et al., 2015). Biochar has been extensively used in environmental applications such as stormwater and wastewater treatment, landfill methane mitigation, and carbon sequestration (Reddy et al., 2014; Xie et al., 2015; Chetri et al., 2022). In a potential composite that includes chitosan and biochar, chitosan can contribute to the contaminant remediation process due to its amine and hydroxyl functional groups, which interact with contaminants through ion exchange, electrostatic, and hydrogen bonding, among other reactions. On the other hand, biochar enhances the opportunities for contaminant adsorption and other reactions by increasing the available number of reaction sites. Furthermore, chitosan-amended bentonite can have similar advantages with the increase in available surface area due to the bentonite and the increase in active functional groups due to the chitosan, which contribute to contaminant adsorption. This work is a comprehensive literature review of studies employing chitosan-bentonite, chitosan-biochar, or chitosan-bentonite-biochar composites to remove different types of contaminants to critically evaluate the potential of a novel composite derived from these materials.

2. Chitosan

Chitosan – a deacetylated biopolymer derivative of chitin (Fig. 1) – is the preferred form of chitin for adsorption applications. Deacetylation removes the acetyl group, CH₃CO, from the chitin polymer chain. This removal process increases the number of active sites and, thus, the adsorption capacity. For example, chitosan has been shown to adsorb 5 to 6 times the amount of dissolved metals compared to chitin (Yang and Zall, 1984). The chitin-to-chitosan conversion process consists of a series of steps: deproteinization, demineralization (e.g., calcium carbonate removal), color removal (bleaching), and finally deacetylation with sodium hydroxide (Kumar, 2000; Rinaudo, 2006; Pal et al., 2021). Degree of deacetylation (DD) refers to the average number of D-glucosamine units per 100 monomers expressed as a percent (Sabnis and Block, 1997). The product is termed chitosan when the DD is at least \sim 50%– 75% (Darder et al., 2003; Rinaudo, 2006; Li et al., 2020). Deacetylation increases the number of potential adsorption sites - amine (-NH2) functional groups and hydroxyl (-OH) groups – along the polymer chain compared to chitin. Chitosan is insoluble in water but soluble in low pH (pH < 6.5) solutions such as dilute organic acidic solutions and hydrochloric acid (Kurita, 2001). The chitosan molecular weight, and thus the

potential number of adsorption sites, depends on the chitin source and procedure used to convert the chitin to chitosan. The average molecular weight of chitosan may range from 3.8×10^3 Da to 2×10^6 Da (Kumar, 2000; Sudha et al., 2017). Chitosan can also be processed into different forms, such as flakes, powder, gel beads, fibers, membranes, nano-fibers, and nano-particles. Both chitin and chitosan are biodegradable, biocompatible, nontoxic, and have significant adsorption properties (Pal et al., 2021). On the other hand, the hydrophobicity of chitosan can be addressed through crosslinking and by modifying the chitosan to form hydrogels (Cohen and Poverenov 2022; Guan et al., 1996; Calvo et al., 1997).

2.1. Chitosan for contaminant removal

The versatility of chitosan and its many derivatives for removing various contaminant species from water and wastewater has been demonstrated in many studies. Previous researchers have shown the effectiveness of chitosan and its derivatives in removing pharmaceuticals (Liakos et al., 2021), proteins (Cheng et al., 2017), dyes (cationic and anionic) (Sadeghi-Kiakhani et al., 2013), endocrine-disrupting compounds (Krupadam et al., 2011), herbicides and pesticides (de Moraes et al., 2013), organic material and suspended solids (dairy waste) (Geetha Devi et al., 2012), phenols (Cheng et al., 2020), fluoride (Davila-Rodriguez et al., 2009), fungicides, humic acid (Dehghani et al., 2018), and hydrocarbons from aqueous solutions (Gentili et al., 2006).

Chitosan and its derivatives can also adsorb a wide range of heavy metals and other cationic and anionic species, including mercury (Ramachandra Nair and Madhavan, 1984; Peniche-Covas et al., 1992), iron (Reiad et al., 2012), zinc (Moghimi, 2014), lead (Aliabadi et al., 2014), nickel (Wang and Kuo, 2008), copper (Wan Ngah et al., 2011), vanadate (Guzman et al., 2002), sulfate, molybdate (Moret and Rubio, 2003), and arsenic (Kwok et al., 2009, 2014) among many others. Several mechanisms by which chitosan removes heavy metals from surrounding fluids have been proposed: ion-pairing, ion exchange, metal chelation, and electrostatic interactions (Aizat and Aziz, 2019; Boddu

et al., 2008). Chitosan contains amine (-NH₂) and hydroxyl (-OH) functional groups along the main chain of the polymer molecule and can remove metal ions from the surrounding fluid through adsorption onto these active sites (Pal et al., 2021; Upadhyay et al., 2021). Furthermore, the hydroxyl and amino groups may act as electron donors, a mechanism called chelation (Muzzarelli, 1983). The metal ion interacts with two amino groups from glucosamine residues on the polymer chain. The amino group acts as the active site at which adsorption takes place due to its lone pair of electrons (Boddu et al., 2008). Chitosan's ability to adsorb metal ions depends on the DD and surrounding fluid pH. The DD determines the number of free amino groups and the hydrophilicity due to the breakdown of the crystalline structure (Kurita, 2001). Metal ion adsorption is a function of pH and increases as pH increases. When the surrounding fluid pH becomes more acidic, positively charged metal ions must compete with hydrogen ions for remaining active sites as the amino groups become protonated (Boddu et al., 2008; Bhatnagar and Sillanpää, 2009).

While chitosan has many advantages for use in adsorption applications (non-toxic, high adsorption capacity, etc.), it also has several undesirable properties. Chitosan has relatively weak mechanical properties (Dotto et al., 2013), typically forming a soft gel-like structure at pH < 5.5 and consequently reducing its material strength (Chiou and Li, 2003; Crini and Badot, 2008). The specific surface area (SSA) is a critical parameter that determines the adsorption capacity of an adsorbent since the adsorption process is a surface phenomenon (Worch, 2012). Chitosan SSA depends on the source, processing, and form (e.g. flake or powder) and is relatively low (Rorrer et al., 1993; Crini and Badot, 2008) with many measured values reported in the literature (e.g., 0.03 $m^2/g - 7.3 m^2/g$; Cestari et al., 2004; Wan Ngah et al., 2005; Uzun, 2006; Vanamudan and Pamidimukkala, 2015; Ardila et al., 2017). Chitosan has low porosity (El-Dib et al., 2016; Wang et al., 2005; Rorrer et al., 1993), and so is not ideal for use in remediation applications in isolation. Countermeasures include physical modification, chemical modification, and/or composite synthesis (Bhatnagar and Sillanpää, 2009; Wan Ngah et al., 2011; Vanamudan and Pamidimukkala, 2015; Upadhyay et al.,

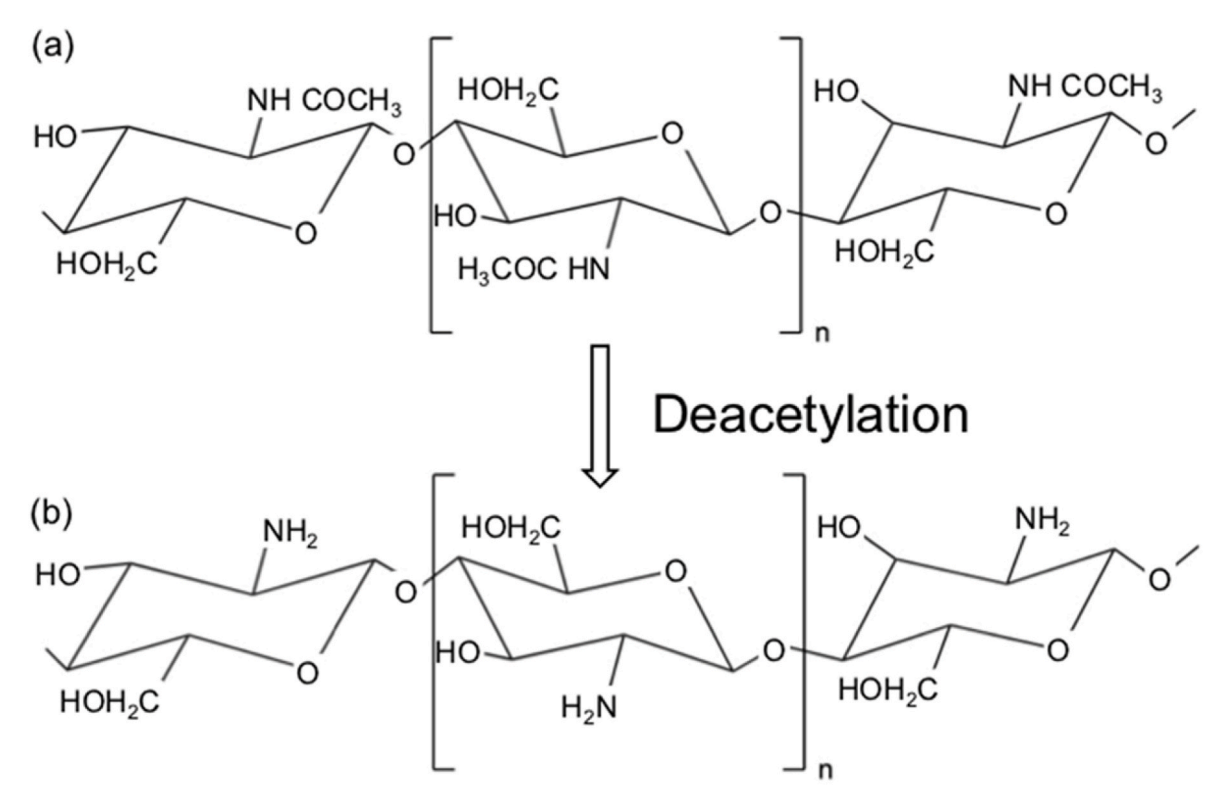


Fig. 1. Structure of (a) chitin and (b) chitosan (after Sudha et al., 2017).

2021). Many chitosan derivatives/composites are chemically modified using crosslinking agents to improve the mechanical properties and chemical stability in acidic or alkaline conditions. However, crosslinking has been reported to reduce chitosan's adsorption capacity. Wan Ngah et al. (2005) reported that chitosan crosslinked with epichlorohydrin (ECH), glutaraldehyde (GLA), and ethylene glycol di glycidyl ether (EDGE) had Fe (II) adsorption capacities of 57.47, 45.25 and 38.61 mg/g respectively, compared to 64.1 mg/g for unmodified chitosan. The study also reported a decrease of Fe (III) adsorption capacity for chitosan from 90.09 mg/g to 72.46 mg/g, 51.55 mg/g, and 46.30 mg/g when crosslinked with ECH, GLA and EDGE respectfully. Cadmium adsorption capacity on GLA crosslinked chitosan decreased from 250 mg/g to 100 mg/g compared to unmodified chitosan (Hsien and Rorrer, 1997). Jóźwiak et al. (2013) observed a reduced adsorption of capacity of cationic basic green dye upon crosslinking chitosan with GLA from 35.64 mg/g to 19.53 mg/g at pH 3, from 476.80 mg/g to 56.10 mg/g at pH 5 and 415.74 mg/g to 137.86 mg/g at pH 9.

3. Chitosan-bentonite composites (CBC)

A cost-effective approach for overcoming the disadvantages associated with unmodified chitosan is binding chitosan to a readily available, low-cost material such as montmorillonite, bentonite, or sand (Zhang et al., 2016). Clay minerals are often selected due to their high adsorption capacity, low cost, wide availability, and mechanical and thermal stability. Their high adsorption capacity stems from the combination of high SSA and ion exchange capacity; adsorption capacity increases with increasing SSA (Ngulube et al., 2017; Upadhyay et al., 2021). Composites are often created to combine the desirable characteristics of chitosan and those of the support material, such as higher strength and increased SSA (Wang et al., 2005; Wan Ngah et al., 2011; Nesic et al., 2012; Ngulube et al., 2017). For example, the tensile strength of a CBC film is 40.5 \pm 1.6 MPa compared to 28.3 \pm 1.2 MPa for a similarly synthesized chitosan-only film (Dotto et al., 2013, 2016). Montmorillonite or bentonite is often used to bind chitosan as it provides structural support, improves chemical stability, improves accessibility to active sites, increases thermal stability, and has high SSA with many available sorption sites (Wang et al., 2005; Wan Ngah et al., 2011). One key advantage of chitosan-clay composites is the ability to adsorb both cationic and anionic species, such as heavy metals and dyes, given the cationic nature of chitosan and anionic nature of montmorillonite particles (Varma et al., 2004; Moussout et al., 2018; Dotto et al., 2016). Additionally, the increased accessible surface area provided by the clay particle broadens the range of the contaminant types that can be removed.

Previous researchers have synthesized many types of chitosanbentonite composites (CBC). CBCs are typically synthesized as custom adsorbents for removing a specific contaminant, e.g., one type of anionic dye, from aqueous solutions. Multisolute systems are rarely studied (Worch, 2012). These studies also highlight adsorption limitations under various conditions, such as the dependency on contaminant concentration, pH, ionic strength, temperature, and the presence of competing molecules and ions (Crini and Badot, 2008; Ngulube et al., 2017). In addition to the relatively simple production process, chitosan-intercalated montmorillonite forms a stable composite structure. The chitosan is essentially irreversibly adsorbed onto the clay particle surfaces. Furthermore, the composite is thermally stable up to ~500 K, which is the combustion temperature of the intercalated chitosan (Darder et al., 2003).

Many other studies include additional synthesis steps to modify the CBC properties to remove selected contaminants. For example, Liu et al. (2015) utilized a cross-linking reaction between chitosan and GLA to enhance the adsorption of an anionic dye (Amido Black 10B). Zhang et al. (2016) modified this cross-linked CBC by mixing the composite in a zirconium oxychloride solution to synthesize a Zr (IV) surface-immobilized cross-linked CBC for increasing the removal of

Amido Black 10B. Nagarpita et al. (2017) grafted chitosan with sodium acrylate and acrylamide, followed by mixing with montmorillonite clay, forming a composite to adsorb one cationic and two anionic dyes. Pereira et al. (2017) utilized a modified clay, montmorillonite KSF, to form chitosan-KSF-montmorillonite beads with sodium tripolyphosphate as a crosslinking agent. The beads were used to remove an anionic dye from the solution. While many studies utilize cross-linking agents and other enhancements to synthesize specialized forms of CBC, this review focuses on the synthesis of unmodified CBC and their applications in contamination removal.

3.1. Materials and synthesis procedures

CBCs are formed by intercalating montmorillonite particles with chitosan molecules. CBCs (Fig. 2) can be readily formed by combining commercially available chitosan and montmorillonite-based clay (bentonite) through solution intercalation techniques. While the specific steps of the synthesis processes found in the literature vary with the goals of the individual studies, common general steps were identified (Darder et al., 2003; Wang et al., 2005; Wang and Wang, 2007; Liu et al., 2015; Dotto et al., 2016). Chitosan is first dissolved in a dilute acidic solution, typically a 1% or 2% acetic acid solution. Under acidic conditions (\leftspH 5), most of the chitosan amine groups are likely to be protonated (Darder et al., 2003). Montmorillonite is mixed with distilled or deionized water at low solids content to produce a slurry. As the montmorillonite particles swell during this hydration step, the interlayer distances increase. The chitosan solution pH is raised to ~pH 5 to minimize mineral dissolution and/or crystalline structure alteration of the clay particles. The two solutions are then slowly mixed. The resulting composite material is separated from the supernatant, washed with distilled/deionized water, and dried. The dried material is then ground to a selected maximum sieve size. A summary of CBC synthesis methods found in the literature is given in Table 1. CBCs may be customized for different applications by varying the (1) chitosan and bentonite types, (2) chitosan: bentonite mass ratio, (3) initial chitosan solution pH, (4) mixing temperature, (5) chitosan-bentonite mixture stirring time, and (6) drying time and temperature.

3.2. Composite material interactions

Researchers have used a variety of techniques to investigate the chitosan-bentonite interaction mechanisms as well as to verify the formation of CBCs. These techniques include Fourier transform infrared spectroscopy (FTIR), X-ray diffraction (XRD), transmission electron microscopy (TEM), and scanning electron microscopy (SEM) (Wang et al., 2005; Darder et al., 2003; Hu Chao et al., 2016; Wang and Wang, 2007; Xiang et al., 2020; Yang et al., 2020).

Utilizing these techniques, two key interactions have been identified as the primary bonding mechanisms between chitosan and montmorillonite, electrostatic interactions and hydrogen bonding. Chitosan is cationic under acidic conditions due to the protonation of the primary amine groups to -NH₃⁺ at pH below the amine pK_a. The protonation of the amine groups also contributes to the ability of acidic solutions to dissolve chitosan. The pKa can vary, ranging from 6.17 to 6.51, depending on the chitosan source, the molecular weight, DD, and surrounding fluid chemistry (solvent, ionic concentration, pH, temperature, etc.) (Wang et al., 2006). Under moderately acidic conditions, the positively charged chitosan amine groups (-NH₃) interact with the negatively charged sites on the montmorillonite particle outer and interlayer surfaces through electrostatic interactions. In addition, chitosan N-H and hydroxyl groups can form hydrogen bonds with the silicate termination sites (Si-O-Si) on the montmorillonite layer surfaces (Darder et al., 2003; Wang et al., 2005; Nesic et al., 2012; Topcu et al., 2018; Yang et al., 2020). Darder et al. (2003) further specified that the initial intercalation of the first layer of chitosan into bentonite is primarily due to electrostatic interactions (chitosan -NH³⁺ and negative

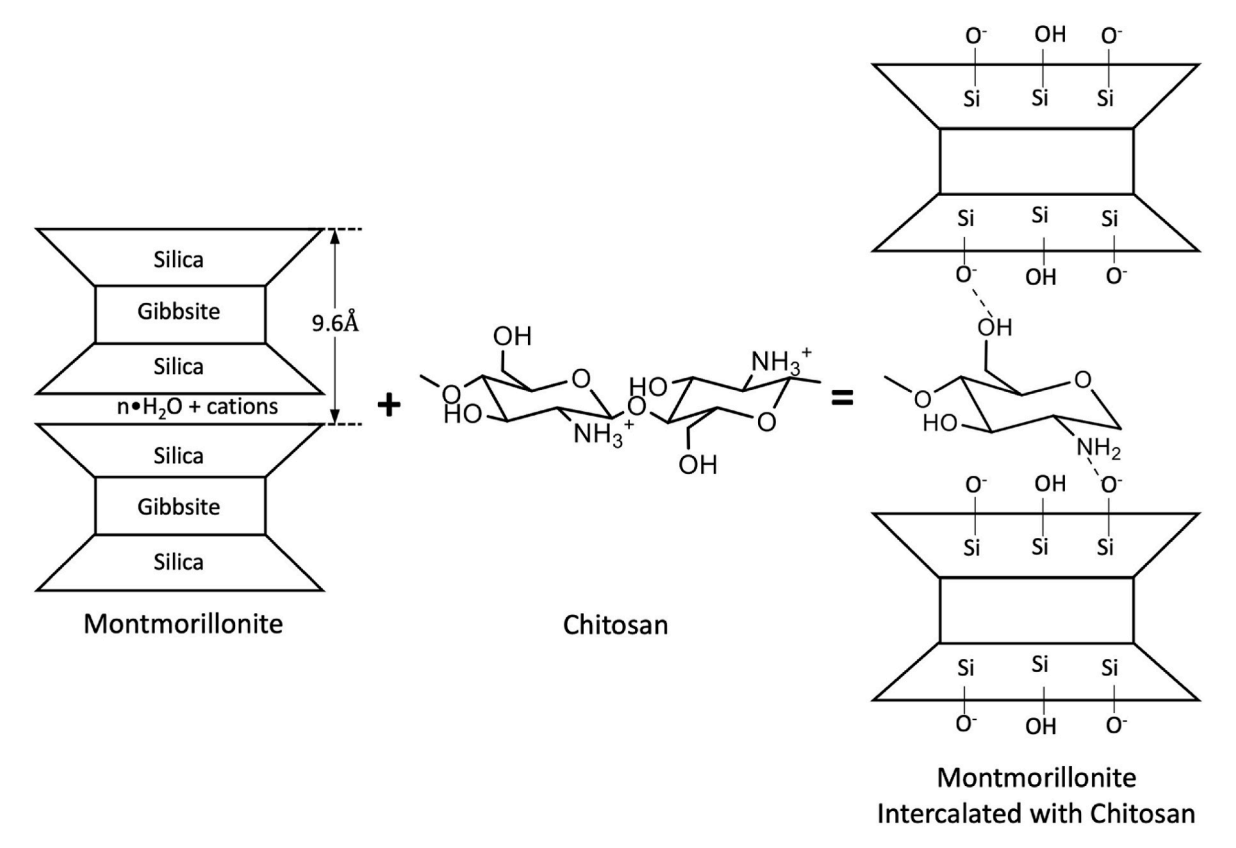


Fig. 2. Intercalation of chitosan into montmorillonite (after Wang et al., 2005).

sites on clay surface), while further adsorption in the interlayer space is primarily due to hydrogen bond formation (chitosan amino and hydroxyl groups with clay mineral surface).

FTIR is often used to identify the chitosan-montmorillonite surface interaction mechanisms by isolating specific bond types. As listed in Table 2, observed characteristic peaks for pure montmorillonite clay are typically attributed to O–H stretching, H–O–H bending, Al–O stretching, Al–OH and Mg–OH vibration, Si–O stretching, Si–O deformation and bending, and O–Si–O asymmetric bending. Chitosan characteristic peaks have been observed due to N–H and O–H stretching, C–H stretching, C–O stretching, O–H bending, and N–H bending (Sellaoui et al., 2018; Jimtaisong and Sarakonsri, 2019; Devi and Dutta, 2017; Yang et al., 2020; Topcu et al., 2018; Darder et al., 2003).

Pure material FTIR spectra are then compared with CBC. Shifts in the characteristic peaks compared to the pure materials indicate bond formation. For example, Jimtaisong and Sarakonsri (2019) compared the FTIR spectra of pure chitosan and CBC. They observed the shift of several peaks from the chitosan spectra to the composite spectra: 3437 cm⁻¹ to 3396 cm⁻¹, 1635 cm⁻¹ to 1630, and 1441 cm⁻¹ to 1530 cm⁻¹. They attributed these observed shifts to the interactions between the chitosan -NH and -OH groups and the bentonite surface -OH groups. Sellaoui et al. (2018) observed shifts in characteristic peaks of -OH stretching for both bentonite and chitosan from 3600 cm⁻¹ (bentonite) and 3456 cm⁻¹ (chitosan) to 3453 cm⁻¹ for the composite, Topcu et al. (2018) observed a shift in the N-H bending vibration from 1560 cm⁻¹ to 1550 cm⁻¹ corresponding to pure chitosan and CBC, respectively. They attributed this shift to the electrostatic interaction between the protonated amine groups and negative sites on the montmorillonite mineral surface. The composite spectra also showed that the frequency bands associated with montmorillonite shifted toward lower frequencies in the composite, which was attributed to electrostatic interactions between the mineral and the chitosan.

X-ray diffraction is commonly used to confirm the intercalation of chitosan molecules into montmorillonite. Yang et al. (2020) observed

that chitosan is a crystalline material with maximum intensity peaks for the pure material at $2\,\theta=20.4^\circ$, while peaks for pure bentonite occurred at $2\,\theta=19.7^\circ$, 26.6° , 29.4° , 35.1° , 54.0° , 61.8° , 73.1° , and 76.4° . Observed shifts in the XRD diffractogram peaks for the CBC – maximum intensity at $2\,\theta=20.0^\circ$ – were attributed to the intercalation of bentonite by chitosan. A decrease in the peak intensity ($2\,\theta$ values) with increasing chitosan-bentonite ratio (increasing the amount of chitosan relative to bentonite) has also been observed by several researchers. This increase in basal spacing was used to confirm the intercalation of bentonite by chitosan (Darder et al., 2003; Wang et al., 2005; Wang and Wang, 2007; Yang et al., 2020).

Scanning electron micrographs reveal differences in the surface morphology of bentonite particles and CBCs. Yang et al. (2020) observed that the CBC appears like bentonite particles with "cotton-like" irregular shapes attached to the outer surfaces. Xiang et al. (2020) also observed rough, irregular surfaces of the CBC compared to pure bentonite. Morphology analysis can be further refined using TEM. Wang et al. (2005) observed individual chitosan intercalated montmorillonite particles ranging in size from 400 to 600 nm. Furthermore, these individual composite particles formed edge-to-edge flocculated at higher montmorillonite mass ratios, which is attributed to hydrogen bond formation between the chitosan amino and hydroxyl functional groups and the clay silicate layers.

3.3. Composite properties

Chitosan-bentonite interactions and composite properties result from the synthesis conditions and procedures. The pH of the chitosan solution before mixing with the bentonite solution, the chitosan: bentonite mass or molar ratio (C:B), and mixing temperature are among the most commonly studied variables for CBC synthesis.

<u>pH:</u> One step in the CBC synthesis is acidifying the chitosan solution to promote dissolution. Acidification results in chitosan protonation, promoting chitosan adsorption onto bentonite surfaces. The maximum

 Table 1

 Chitosan-bentonite composite synthesis methods based on selected studies.

Application	Chitosan	Bentonite	Chitosan solution preparation	Bentonite suspension preparation	Chitosan-Bentonite composite preparation	Reference
Congo Red (anionic dye) removal	Chitosan (LMW) Source: NS MW: 9 × 10 ⁵ g/mol DD: 85%	Montmorillonite (MMT) CEC: 76.4 mequiv/ 100 g	 Chitosan dissolved in 1% (v/v) acetic acid solution. Solution pH adjusted to 4.90 using 20 wt% NaOH 	MMT hydrated in 100 mL distilled water.	Chitosan solution slowly added to MMT suspension and stirred at 60 °C for 6 h. Composite is washed with distilled water until pH of the supernatant reaches 7.00. Composite is dried at 60 °C for 12 h.	Wang and Wang (2007)
Composite Synthesis	Chitosan (MMW) Source: NS MW: 9.27 × 10 ⁵ g/ mol DD: 82.5%	Montmorillonite CEC: 92.7 mequiv/ 100 g	 Chitosan dissolved in 2% (v/v) acetic acid solution at 2 wt % and centrifuged to remove insoluble material. 	Montmorillonite hyudrated in distilled water.	 MMT suspension added to chitosan solution and stirred at 60 °C for 6 h. MMT-chitosan solution kept at 60 °C for 48 h. After drying, the film is soaked in 1 M NaOH for 5 h to neutralize acid. Film rinsed with distilled water and dried at 60 °C for 24 h. 	Wang et al. (2005)
Chitosan-based electrode synthesis for detection of anions.	Chitosan (HMW) Source: NS MW: 3.4 × 10 ⁵ g/mol DD: 75%	Sodium montmorillonite CEC: 76.4 mequiv/100 g	 Chitosan dissolved in 1% (v/v) acetic acid and stirred for 4 h. Solution pH of the solution adjusted to 4.90 using NaOH. 	Sodium Montmorillonite hydrated in bi-distilled water.	 Chitosan solution slowly added to MMT suspension, stirred for 2 days. Composite washed with distilled water until the free from acetate. Composite air-dried at 50 °C. 	Darder et al. (2003)
Anionic and cationic dye removal from wastewater	Chitosan Source: NS MW: 9 × 10 ⁵ g/mol DD: 80%	Bentonite CEC: NS	 1 g chitosan is dissolved in 100 mL of 1% (w/v) acetic acid solution and stirred at 45 °C for 2 h. Solution pH adjusted to 5.0 using 0.1 mol/L⁻¹ NaOH. 	- 1 g bentonite hydrated in 100 mL deionized water under magnetic agitation at 60 $^{\circ}\text{C}$ for 5 min.	 Chitosan solution and bentonite suspension mixed and stirred at 60 °C for 4 h. Composite oven-dried at 60 ± 2 °C for 20 h. 	Dotto et al. (2016)
Adsorbent of Bezactiv Orange V-3R dye	Chitosan Source: NS MW: (1–3) × 10 ⁵ g/ mol DD: 80%	Montmorillonite	- Chitosan (1 wt%) dissolved in 0.2 M acetic acid at 50 °C.	- MMT dissolved in 0.2 M acetic acid at 50 $^{\circ}\text{C}$ with continuous stirring for 30 min.	Chitosan solution and MMT suspension are mixed while stirring for 30 min. Resulting solution poured onto petri dishes and allowed to evaporate at room temperature for 24 h.	Nesic et al. (2012)

Note: Abbreviation used: MW - molecular weight; DD - degree of deacetylation; MMT - montmorillonite; CBC - chitosan-bentonite composite; CEC - cationic exchange capacity; HMW - high molecular weight; LMW - low molecular weight; MMW - medium molecular weight; NS - not specified.

amount of chitosan on the montmorillonite surface can be estimated based on the percentage of protonated amine groups at a given pH (known pKa) and the montmorillonite cation exchange capacity, assuming primarily electrostatic interactions between the chitosan and montmorillonite. Darder et al. (2003) estimated the adsorption capacity of bentonite clay (Clay Minerals Society) with commercially available chitosan by theoretically calculating the cation exchange sites on the clay surface and the equivalent -NH3+ of the polymer that could be adsorbed and found it to be 107.2 meq/100 g at pH 5. However, the Langmuir fit for the adsorption studies at pH 5 showed the adsorption capacity to be greater, 187.4 meq/100 g. The excess chitosan adsorption was attributed to multilayer adsorption in the clay particle interlayer space. Wang et al. (2006) reported that the pKa value of chitosan is around 6.51 to 6.39, regardless of molecular weight. Hu Chao et al. (2016) found that at a pH of 5.5, the quantity of low and medium-molecular-weight chitosan adsorbed onto montmorillonite was 0.203 mg/mg and 0.190 mg/mg, respectively. Dotto et al. (2016) found that the swelling of CBC composite with a C:B mass ratio of 5:1 increased with decreasing pH (pH 9-3) up to 1100% at pH 3. This was attributed to the repulsion between protonated chitosan amino groups under acidic pH conditions, which allowed for more fluid to enter the interlayer space. Further, swelling occurred rapidly, with maximum swelling reaching less than 20 min. They hypothesized that this swelling response contributes to the adsorption capability of the composite.

3.3.1. Chitosan: bentonite mass/molar ratio

Several studies have reported the effect of C:B (mass or molar ratio) on composite properties (Wang and Wang, 2007; Koutsopoulou et al., 2020; Darder et al., 2003, among others). Increasing C:B results in increased adsorption of chitosan by bentonite, increased intercalation, and at lower C:B ratios (relatively high masses of bentonite), increasing flocculation of the composite particles (Wang et al., 2005; Wang and Wang, 2007). In addition, the final composite volume, density, and SSA tend to decrease with increasing chitosan percentage, while the pore size tends to increase with increasing chitosan percentage (Darder et al., 2003; Wang and Wang, 2007).

3.3.2. Temperature

Yu et al. (2018) studied the effect of temperature on chitosan adsorption in bentonite. Their results showed that increasing temperature (30–50 $^{\circ}\text{C}$) decreased the chitosan loading from 121.48 to 55.98 mg/g. The movement of chitosan molecules increases due to increasing temperature in the solution, which may result in chitosan desorption and loading of chitosan on bentonite surfaces.

3.4. Contaminant removal – capacities and mechanisms

While both unmodified and modified CBCs have been studied to investigate the potential for contaminant removal from waste and

Table 2Wave numbers corresponding to bentonite, chitosan, and chitosan-bentonite interactions obtained with FTIR.

Surface Group	Wavenumber(s) (cm ⁻¹)							
	Bentonite	Chitosan	CBC					
O–H stretching	3600, 3466, 3621, 3742, 3440, 3627, 3630	3456, 3437, 3446, 3445-3284, 3440, 3451, 3449, 3450, 3300	3453, 3397, 3440, 3388, 3445, 3622, 3621					
O–H bending	919	1646						
H–O–H bending	1636, 1633, 1640, 1641							
Al-O stretching Al-OH, Mg-OH vibration Al-O-Si deformation	918, 619, 618 848, 729, 913, 3635, 843, 793 515		917, 914 915, 624, 842, 792					
C–H stretching		2924, 2921, 2920, 2868, 2890, 2929, 2874, 2900	2923, 2856					
C–H bending		1379, 1385, 1425, 1401	1300, 1450, 1425					
C–H deformation vibrations		1416, 1374, 1312, 1400	1419, 1375					
C–O stretching		1150, 1054, 1023, 1150-1000, 1633, 1645, 1138, 1095	1630, 1634					
Amide and		1625, 1635, 1655,	1638, 1630, 1644,					
C=0		1650, 1740, 1540,	1640, 1645, 1519,					
stretching		1650, 1535, 1540, 1650	1524					
N–H stretching		1441, 3437, 3446, 1420, 3445-3284, 3370, 3300	1530, 3397, 3388, 1531–1541, 1550					
N–H bending		1560, 1540, 1651, 1560, 1590	1550, 1560, 1612, 1566					
C-N stretching		1485	1503					
C–O–C bending		1149, 1152						
С-ОН		1081						
stretching	1044 1101 1020		1049 1090 1004					
Si–O stretching	1044, 1191, 1039, 1006, 1000, 1118-		1048, 1089, 1004, 1044, 1050, 1086,					
	1040, 1080, 1087, 1035, 1000		1034					
O-Si-O	825		817, 819					
asymmetric stretching			,					
Si–O,	709, 526, 746, 507,		715, 701, 520,					
deformation	515, 450, 523, 520,		467					
and bending	467							
O–Si–O asymmetric bending	503		510, 505					

Selected data from Darder et al. (2003), Sellaoui et al. (2018), Jimtaisong and Sarakonsri (2019), Devi and Dutta (2017), Topcu et al. (2018), Yang et al. (2020), Wang and Wang (2007), Nesic et al. (2012), Moussout et al. (2018), Hu Chao et al. (2016), Dotto et al. (2016), Günister et al. (2007), Devi and Dutta (2017), Celis et al. (2012).

ground waters (Syafalni et al., 2012; Tan et al., 2015; El-Dib et al., 2016; Aizat and Aziz, 2019; Cheng et al., 2020; Binaeian et al., 2020), heavy metals (Wan Ngah et al., 2004, 2005, 2011; Budnyak et al., 2016; Muliwa et al., 2018; Foroutan et al., 2020; Jia et al., 2021); adsorption of dyes (Wang and Wang, 2007; Liu et al., 2015; Zhang et al., 2016; Tan et al., 2015; Dotto et al., 2016; Hu Chao et al., 2016; Pereira et al., 2017; Nagarpita et al., 2017; Vanamudan and Pamidimukkala, 2015) removal of humic acid (Dehghani et al., 2018), and remediation of metal contaminated soil (Kumararaja et al., 2018), this review focuses on unmodified chitosan-bentonite composites (CBC) for contaminant removal and the corresponding interaction mechanisms.

3.4.1. Dye removal

Many studies have focused on removing dyes from solution (usually water) using CBCs. The most common dye pollutants are water soluble and have a net charge, either cationic or anionic, which contributes to the difficulty in their removal. Removal of Congo Red, an anionic dye, is one example of investigating the efficacy of CBC for remediation of contaminated water since its anionic nature inhibits adsorption onto negatively charged clay mineral surfaces. Wang and Wang (2007) studied the potential of CBC for absorbing Congo Red and reported that the average absorption capacity for CBC is higher than either chitosan or bentonite alone. They observed that Congo Red adsorption increased with increasing chitosan percentage (C:B = 1:10 to 1:1), decreasing pH (pH 4-9), increasing temperature (30°-50 °C), and increasing contact time (0-600 min). They attributed the interaction between the Congo Red molecules and CBC to electrostatic interactions (chitosan -NH₃ groups interacting with negative clay mineral sites at acidic pH), chemisorption, and endothermic adsorption. Xiang et al. (2020) investigated the removal of Methyl Red, an anionic dye, with CBC. They found that for 2.5 mg/L Methyl Red, adsorption increased with decreasing pH (pH 1-6) and increasing composite loading (20-70 mg CBC). However, the removal rate increased with increasing C:B mass ratio (0.04-0.12 w/w) up to a maximum value of 0.08 and then decreased at higher mass ratios. However, Nesic et al. (2012) observed different trends. They studied the absorption of Bezactiv Orange V-3R (anionic) dye on chitosan-montmorillonite membranes. The membranes were created with varying percentages of clay, ranging from 10% to 50%. At a concentration of 80 mg/L dye, adsorption capacity increased with increasing clay content, increasing pH (pH 4-7.5) up to pH 6, and decreasing temperature (8°-55 °C).

Dotto et al. (2016) developed a CBC with a C:B mass ratio of 5:1 to remove an anionic dye, Amaranth Red, and a cationic dye, Methylene Blue, from aqueous suspensions. Solution pH had different impacts on the adsorption of the two dyes due to their opposite charge. While increasing pH (pH 2–10) resulted in increasing adsorption of Methylene Blue (maximum adsorption capacity at pH 10 496.5 mg/g) by the CBC, decreasing adsorption was observed for Amaranth Red with optimum adsorption conditions at pH 2 (362.1 mg/g). For both dyes, increasing solution temperature (25°-55 °C) decreased adsorption, with the adsorption capacity of Methylene Blue exceeding that of Amaranth Red. Another significant observation made by Dotto et al. (2016) was that their CBCs exhibited recharge capability – adsorption of Amaranth Red was possible for three cycles and Methylene Blue for two cycles.

Wang and Wang (2007) listed two potential mechanisms for the adsorption of anionic dye on CBCs: (1) electrostatic attraction between protonated chitosan groups in the CBC and the dye and (2) chemical reactions between the adsorbate and adsorbent. Below pH 6.3, the pKa of amine groups (-NH₂) in the chitosan structure becomes protonated as -NH³⁺, facilitating the anionic dye adsorption. At lower pH values, the adsorption is primarily controlled by the ion exchange mechanism. Yang et al. (2020) stated that at pH < 6, chitosan in the CBCs becomes protonated, forming $-OH^{2+}$ and $-NH^{3+}$, which leads to electrostatic attraction between the CBC composite and negatively charged ions. Dotto et al. (2016) suggested that for cationic dyes at higher pH, the Si–O groups become Si–O $^{-}$, which interacts with the positively charged sites on the cationic dye molecule.

3.4.2. Heavy metal removal

Moussout et al. (2018) compared the Cr (VI) removal capacity of a CBC synthesized at a very low percentage of bentonite (45:1 C:B) with pure chitosan. The optimum adsorption capacities for Cr (VI) ions occurred at a pH of 5 and a temperature of 25 °C (304 mg/g for pure chitosan and 223 mg/g for CBC). Under acidic pH conditions, the amino groups (–COONH₂) and –OH groups become protonated as –COONH $_3^+$ and H $_1^+$ in the CBC composite, which interact with negative CR(VI) species (HCrO $_4^-$, CrO $_4^-$, CrO $_7^-$) through Coulombic attraction. Liu et al. (2022) investigated Cr(VI) removal from contaminated soil with CBCs.

They observed a significant reduction in the levels of exchangeable fraction and oxidizable fraction in the soil. The concentration of residual fraction increased from 0.24 mg/kg to 49.82 mg/kg, resulting in a decreased availability of chromium for biological processes. Senol and Simsek (2022) studied the adsorption of Pb²⁺ ions on chitosan-bentonite beds. They found the removal rate to be 95% at pH of 4.5. The –OH, –NH₂, and –NH–CO–CH₃ groups also work as chelating agents for capturing other heavy metals (Kumararaja et al., 2018).

3.4.3. Groundwater and wastewater treatment

Many types of contaminants may exist in groundwater and wastewater, including heavy metals, ionic dyes, and humic acid. Chitosanclay composites are particularly effective for contaminant removal from wastewater due to their ability to adsorb contaminants through physical and chemical mechanisms (Biswas et al., 2021). Bleiman and Mishael (2010) synthesized CBCs to remove selenium from well water. The composites were able to remove 98% of the selenium present in the well water (initial Se concentration = 1.396 mg/L). Syafalni et al. (2012) investigated using chitosan and bentonite as coagulants for raw water treatment. They found that at pH 6.8, the treatment removed 98% of turbidity, resulting in high-quality water with 10 TCU color units, 1.38 NTU turbidity, 0.01 mg/L chlorine and aluminum. Yee et al. (2019) studied the potential of chitosan-coated bentonite for arsenic removal from groundwater. They found the temperature of 55 °C to be favorable for As(V) removal. The maximum adsorption capacity chitosan-coated bentonite for arsenic was found to be 1.47 mg/g. The negatively charged bentonite can enhance flocculation to bind individual composite particles forming larger flocs (Pan et al., 1999). In groundwater, arsenic may be present in several forms such as H₂AsO₄, $HAsO_4^-$, and AsO_4^{3-} . The adsorption of As (V) is facilitated by -OH and -NH₂ groups of the CBC composite (Yee et al., 2019).

4. Chitosan-biochar composites

4.1. Materials and synthesis procedures

Biochar, a carbonaceous material, is used extensively in environmental applications. The applicability and the capacity of contaminant removal of biochar depend on its properties such as SSA, pore volume, and functional groups on the surface of the biochar. These properties of biochar vary vastly based on the source feedstock used, production conditions, and pre-and post-production treatments, if any (Oni et al., 2019). Generally, biochars are produced by pyrolysis of waste biomass in oxygen deficient conditions at high temperatures and employing different heating rates. The properties of the composite produced from biochar and chitosan thus vary depending on the type of chitosan and biochar used and the synthesis procedure followed. These differences in properties affect the contaminant removal capacities of the composites. Thus, the material properties and synthesis procedure chitosan-amended biochar (CAB) are crucial in understanding the contaminant removal capacities. Properties of chitosan and biochar used in different studies, reporting the use of CAB for contaminant removal applications, are presented in Table 3.

CABs have previously been synthesized and studied for use in contaminant adsorption applications. The synthesis steps followed by different studies to synthesize CABs are summarized in Table 3. The composite synthesis procedure, followed in many of these studies, consists of four common steps: (1) A chitosan solution is prepared by dissolving chitosan in acetic acid (2) biochar is then mixed with the chitosan solution to create a suspension (3) the suspension pH is then adjusted using NaOH and (4) the solids are separated from the suspension and dried for further experiments. A schematic of the general synthesis procedure followed in most of the studies reviewed is presented in Fig. 3.

Chitosan in its original form is not soluble in water. Hence, a weak acid, such as acetic acid, is typically used as a solvent. The suspension

pH is typically increased by adding NaOH to minimize chitosan dissolution. The suspended solids are then filtered out and washed with deionized water/distilled water to remove any excess NaOH. In addition to these steps, several other studies have used additional steps in preparing the composite to obtain composites of desired properties. Crosslinking agents such as dimethyl formamide (DMF), ethylene diamine tetra-acetic acid (EDTA), and ECH, have been used to enhance the functionality of the resulting composite (Zheng et al., 2020; Manyatshe et al., 2022). In several studies, biochar was modified with metal amendments such as ferric chloride (FeCl₃) for synthesizing a composite with magnetic properties for immobilizing heavy metal contaminants (Palansooriya et al., 2021). This review focuses on studies that synthesized CAB using chitosan and biochar only.

4.2. Composite material interactions

Few studies have performed the microstructural and morphological characterizations to understand the interactions between chitosan and biochar in CAB. The CAB's external morphology was rougher when compared to biochar alone (Afzal et al., 2018). SEM images of the composite indicated some crystalline substances on the surface and in the pores of the biochar, which was reported to indicate that chitosan is not only deposited on the surface of the biochar but entered the biochar pores as well, affecting its pore structure (Shi et al., 2020). FTIR studies on the composites indicate changes in the functional groups due to the deposition of chitosan onto the biochar surface. Introducing of new bands in the CAB FTIR spectra produced from pomelo biochar compared to biochar alone was reported to stretch C-H, C-O, and C-O-C bridges. Greater peaks corresponding to -NH2 were inferred as increased amine groups on the biochar surface (Afzal et al., 2018). Dewage et al. (2018) observed similar stretching for composite produced from pyrolyzed pinewood biochar. Pinewood biochar produced from gasification had bond stretching that indicates the addition of C-H, -CH, and CH2 from the chitosan. Bond stretching corresponding to unhydrolyzed amide functional groups remaining in chitosan has also been reported (Burk et al., 2020). In the composite produced from the biochar of moringa oleifera seeds, Roy et al. (2022) observed peaks that were attributed to -NCO and -CN bonds. These bonds are reportedly formed between the amine group on the chitosan and the carboxyl groups on the biochar surface. Song et al. (2021) performed XRD analysis to confirm the interactions between chitosan and sludge-based biochar. They observed a decrease in the location of the peaks (2 θ) in the composite compared to chitosan alone, indicating the success of composite synthesis.

4.3. Composite properties

Adding chitosan to biochar alters several key properties that influence the adsorption capacity. These properties include surface area, surface charge, and the available functional groups. The adsorption characteristics of biochar are mainly attributed to oxygen functional groups on the surface and the negative surface charge (Dai et al., 2021). Chitosan adds amine and hydroxyl groups on the biochar surface, further enhancing the biochar contaminant adsorption characteristics. In addition, the total surface area and charge are also altered. These changes in biochar properties relevant to contaminant adsorption when combined with chitosan, as reported in the literature, are presented in the subsequent sections.

4.3.1. Surface area

The surface area of an adsorbent significantly influences the adsorption capacities and adsorption mechanisms (Gao et al., 2022). Typically, biochar has a large surface area, making it suitable for adsorption of various contaminants. Despite minimal functional groups on its surface, biochar has high adsorption capacity due to its SSA and pore volume (Qiu et al., 2021). However, when combined with chitosan as a composite, the biochar surface area reportedly decreased. Burk et al.

 Table 3

 Chitosan-biochar composites synthesis methods based on selected studies.

Application	Chitosan	Biochar feedstock	Biochar preparation			Chitosan-biochar composite preparation			Reference
			Pre- treated	Pyrolysis/ Gasification conditions	Post- treated	Chitosan Solution Preparation	Biochar and Chitosan Mixing	pH Adjustment and Extraction	
Ciprofloxacin adsorption	Commercially acquired DD: NR MW: NR	Pomelo peels	Yes ^a	Temperature increased to 450 °C and maintained for 15 min.	Yes ¹	1 g of chitosan in 60 mL acetic acid (2%)	1 g of the biochar added to the solution. Stirred for 30 min.	Suspension added dropwise into 200 mL of NaOH (2.5%) and kept for 12 h. Washed and dried.	Afzal et al. (2018)
DOM removal from wastewater	Commercially acquired chitosan DD: 95% MW: NR	Wheat straw		$700~^\circ$ C for 1hr under N_2 environment	Yes ²	3 g of chitosan in 250 mL acetic acid (2%)	5 g of the biochar added to the solution. Stirred at 200 rpm for 30 min.	NaOH (2 M) added dropwise to the mixture until the pH reached 8. The mixture was kept for 12 h. Washed with ultrapure water. Dried in oven at 70 °C.	Shi et al. (2020)
Phloridzin adsorption	Commercially acquired chitosan DD: 95% MW: NR	Apple branches	Yes ^b	300 °C at a heating rate of 10 °C/min for 2 h N_2 environment	No	3 g of chitosan in 500 mL acetic acid (2%)	Prepared biochar added to the solution. Stirred for 1.5 h.	NaOH (1 M) added to the mixture until the pH reached 9. Stirred for 1 h. Oven dried at 80 °C.	Ma et al. (2021)
Sorption of metals from oils sands process water	Commercially acquired chitosan DD: NR MW: NR	Sewage treatment sludge	No	600 °C for 2h at the rate of 10 °C/min under $\rm N_2$ environment	Yes ³	1.05 g of chitosan in 50 mL acetic acid (2%)	0.45 g of biochar added to the mixture. Stirred for 30 min.	20 mL of NaOH solution (2 M) added dropwise to the mixture and stirred for 2 h and kept at 140 °C for 10 h. Washed with DI water and dried at 70 °C.	Song et al. (2021)
Removal of cadmium from aqueous solution	Commercially acquired chitosan DD: 90% MW: NR	Kiwi branch	Yes ^c	$500~^\circ\mathrm{C}$ in a vacuum tube furnace under N_2 environment	Yes ⁴	5.0 g of chitosan in 250 mL acetic acid (2%)	5.0 g of biochar added to the mixture. Stirred for 60 min.	1500 mL NaOH (1%) solution was added dropwise into the suspension, kept for 24 h. Washed and dried.	Tan et al. (2022)
Methylene blue adsorption	Commercially acquired chitosan DD: NR MW: NR	Moringa Oleifera seeds	Yes ^d	350 °C with a heating rate of 5.8 °C/min at 2 bar pressure for 3 h under N ₂ environment	Yes ⁵	1 g of chitosan in 180 mL acetic acid (2%)	3 g of the prepared biochar added to the solution. Stirred for 30 min.	Suspension added dropwise into a 900 mL NaOH (1.2 %) solution and kept in the solution for 12 h. Washed with deionized water. Oven-dried for 24 h at 105 °C.	Roy et al. (2022)
Cadmium adsorption	Commercially acquired chitosan DD: NR MW: NR	Bamboo	Yes ^e	900 °C for 4 h at an N_2 flow of 100 mL/min.	Yes ⁶	0.4 g of chitosan mixed with 2 g biochar in 30 mL of water.	The mixtures stirred with sonication for 2 d at 30 °C and 75% relative humidity.	Separated by vacuum filtration. Oven dried at 100 \pm 5 °C.	Huang et al. (2022)
Heavy metal sorption	Commercially acquired chitosan DD: NR MW: 100–300 kDa	Bamboo, Sugarcane bagasse, Hickory wood, and Peanut hull	No	600 °C at 2 h under N ₂ environment	Yes ⁷	3 g of chitosan in 180 mL acetic acid (2%)	3 g of the as-is biochar added to the solution. Stirred for 30 min.	Suspension containing chitosan and biochar is added dropwise into a 900 mL NaOH (1.2%) solution and kept for 12 h. Washed with deionized water to remove the excess of NaOH. Oven-dried for 24 h at 70 °C.	Zhou et al. (2013)
Lead sorption	Commercially acquired chitosan DD: 85% MW: NR	Pinewood	No	425 °C for 20–30 s	Yes ⁸	3 g of chitosan in 180 mL acetic acid (2%)	3 g of the as-is biochar added to the solution. Stirred for 30 min.	Suspension containing chitosan and biochar is added dropwise into a 900 mL NaOH (1.2%) solution and kept for 12 h.Washed with deionized water to remove the excess of NaOH.Oven-dried for 24 h at 70 °C.	Dewage et al. (2018)

(continued on next page)

Table 3 (continued)

Application	Chitosan	Biochar feedstock	Biochar preparation			Chitosan-biochar composite preparation			Reference
			Pre- treated	Pyrolysis/ Gasification conditions	Post- treated	Chitosan Solution Preparation	Biochar and Chitosan Mixing	pH Adjustment and Extraction	
Cadmium sorption	Commercially acquired chitosan DD:NR MW: 190 kDa	Peanut shell	Yes ^f	Slow pyrolysis at 450 °C for 4 h at a heating rate of 10 °C/min	No	3 g of chitosan in 180 mL acetic acid (2%)	3 g of the as-is biochar added to the solution. Stirred for 30 min.	Suspension containing chitosan and biochar is added dropwise into a 900 mL NaOH (1.2%) solution and kept for 12 h.Washed with deionized water to remove the excess of NaOH.Oven-dried for 24 h at 70 °C.	Shabani et al. (2019)
Cadmium and copper removal from water	Commercially acquired chitosan flakes DD: 85% MW: NR	Pine wood biochar	No	Gasification at 700–900 °C under nitrogen flow with a residence time of 5–10 s	No	3 g of chitosan in 180 mL acetic acid (2%)	3 g of the as-is biochar added to the solution. Stirred for 30 min.	Suspension containing chitosan and biochar is added dropwise into a 900 mL NaOH (1.2%) solution and kept for 12 h.Washed with deionized water to remove the excess of NaOH.Oven-dried for 24 h at 70 °C.	Burk et al. (2020)
Methyl Orange adsorption	Chitosan prepared in lab from shrimp shell waste DD: NR MW: NR	Raw rice husk from local rice-milling factory in the Mekong Delta	No	500 °C, with a heating rate of 10 °C/min for 2 h	Yes ⁹	3 g of chitosan in 180 mL acetic acid (2%)	3 g of the as-is biochar added to the solution. Stirred for 30 min.	Suspension containing chitosan and biochar is added dropwise into a 900 mL NaOH (1.2%) solution and kept for 12 h.Washed with deionized water to remove the excess of NaOH.Oven-dried for 24 h at 70 °C.	Loc et al. (2022)

Note: Chitosan sources not reported in all but one cited study listed here. All the concentrations are reported on volume to volume basis; **Abbreviations:** NR – not reported, DOM – Dissolved organic matter, DD – Degree of deacetylation, MW – Molecular weight; **Pre-pyrolysis/gasification treatment of biochar:** Cut into small pieces and placed in the muffle furnace; Dried branches were ground, passed through sieve #80; Branched were chopped, washed, and dried; Dried and washed with pure ethanol to wash the inorganic impurities. Dried at 50 °C for 12 h; Washed with deionized water three times to remove the dirt contained in the samples. Air-dried, chopped into a particle size $1.0 \times 1.0 \times$

(2020) observed a significant reduction in surface area from 34.1 to $4.61~\text{m}^2/\text{g}$ of biochar compared to the CAB. The surface area reduction depends on the biochar type and the fraction of chitosan in the composite (Zhou et al., 2013; Loc et al., 2022; Zheng et al., 2020). This decrease is generally attributed to chitosan filling the biochar pores (Burk et al., 2020; Zhou et al., 2013). However, a composite produced from bamboo biochar was reported to have no significant change in the surface area compared to pure biochar (Huang et al., 2022). Except in a few cases among the studied literature, most studies that reported changes in surface area reported a decrease in the surface area in CAB composite compared to biochar alone. Yet, this decrease in surface area had no adverse effect on the adsorption capacities due to the additional chitosan functional groups in most of the studies based on the reported capacities.

Few studies included additional steps in synthesizing CAB, such as cross-linking and magnetizing the composite, to increase the surface area. For example, Manyatshe et al. (2022) observed an increase in sugarcane bagasse biochar-chitosan composite surface area compared to pure biochar. They attributed this increase to ECH used as a crosslinking agent in the composite synthesis since the composite produced without the crosslinking agent saw no change in the surface area.

4.3.2. Carbon to nitrogen ratio

The composite carbon-to-nitrogen(C/N) ratio indicates the amount of chitosan deposited onto the biochar surface. The ratio is reportedly significantly lower for CAB than biochar alone (Zhou et al., 2013). Burk et al. (2020) used the increase in nitrogen content to determine the weight ratio of the chitosan to composite. They found that the composite consisted of only 25% chitosan even though it was synthesized at a ratio of 1:1 chitosan: biochar. This result is also consistent with other studies, which reported only a percentage of the added chitosan in the synthesis remaining on the biochar surface (Dewage et al., 2018; Zhou et al., 2013).

4.3.3. Surface charge

Contaminants with charge are adsorbed predominantly by electrostatic interactions. Surface charge of the adsorbent dictates the adsorption capacity in such cases. The pH at which the surface charge of the adsorbents becomes zero is the point of zero charge (PZC). For chitosan, when the pH of the surrounding aqueous solution is lower than the PZC, protonation of the hydroxyl and amine groups renders the net surface charge positive (Loc et al., 2022). The PZC for chitosan depends on the type of chitosan. Kwok et al. (2014) reported a PZC of 8.3 and 9.03 for various chitosan types. For the biochar, the PZC is generally in the acidic range (pH < 7), implying the surface charge of biochar is

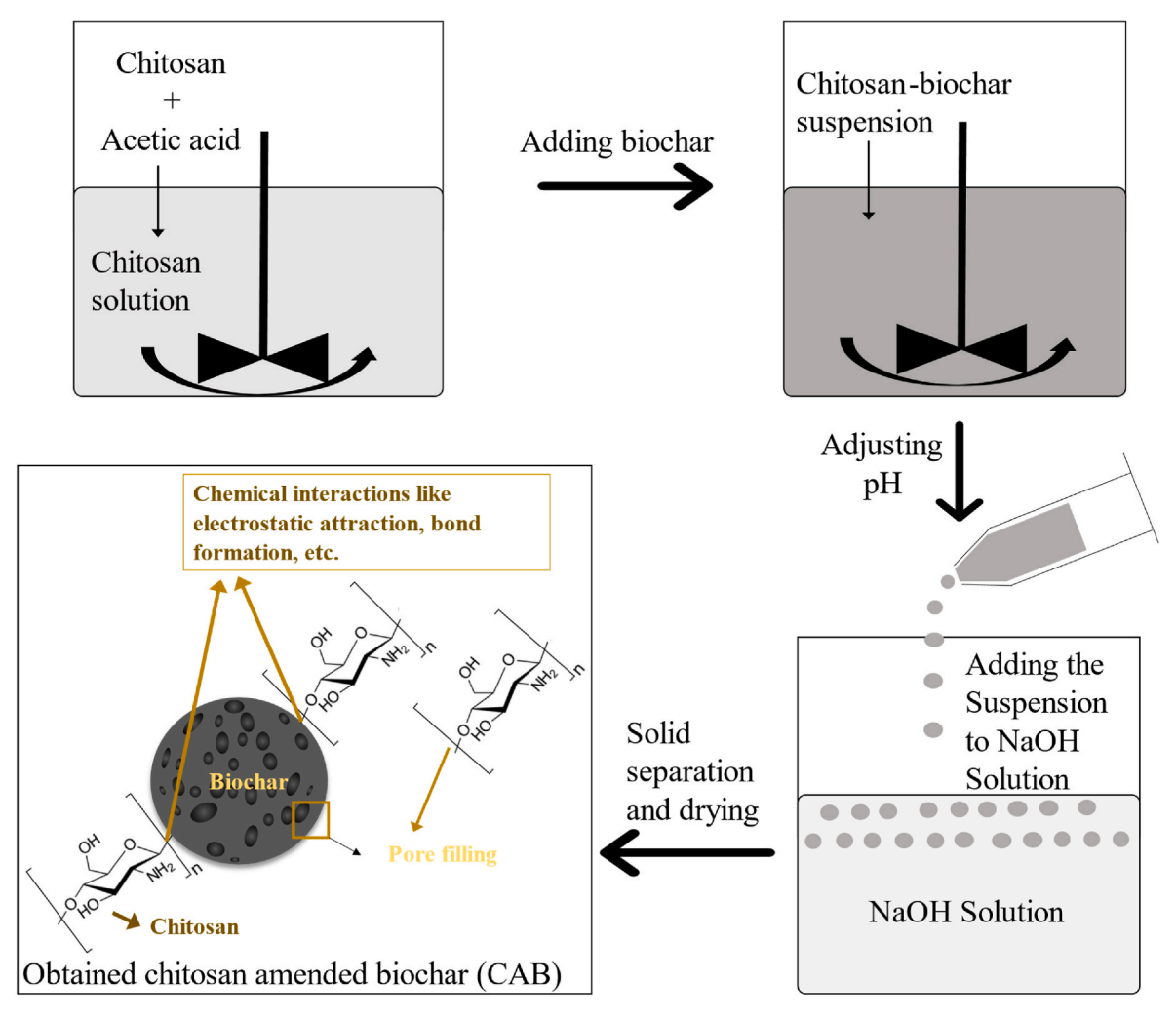


Fig. 3. Synthesis process for chitosan-amended biochar commonly followed in the reviewed studies.

negative at neutral pH. For CAB, adding the amine and the hydroxyl groups from chitosan generally decreases the negative surface charge of biochar, thus increasing the PZC. The increase in PZC also indicates that the adsorption of the chitosan onto the surface of biochar is through electrostatic interactions (Huang et al., 2022).

A major factor affecting the surface charge of biochar is the pH as discussed above. The pH of CAB composites as reported by Zhou et al. (2013), was observed to be higher than the biochar pH from which the composites were derived. Composites synthesized from chitosan and bamboo biochar (pH 7.9 to pH 8.2), sugarcane bagasse biochar (pH 7.5 to pH 8.1), hickory wood biochar (pH 8.4 to pH 8.6), and peanut hull biochar (pH 6.9 to pH 7.3) were reported to have an increase in pH when compared to their corresponding biochars (Zhou et al., 2013). The increase in pH is also due to the deposition of amine groups on biochar. Such increases in pH can also alter the surface charge of the composite affecting the adsorption of various ions by the composite.

4.4. Contaminant removal - capacities and mechanisms

Past studies on CABs evaluated their removal efficiencies of heavy metals, dyes, and dissolved organic matter, among other contaminant types, as shown in Table 3. This section briefly summarizes the results obtained from these studies regarding adsorption capacities and predominant adsorption mechanisms.

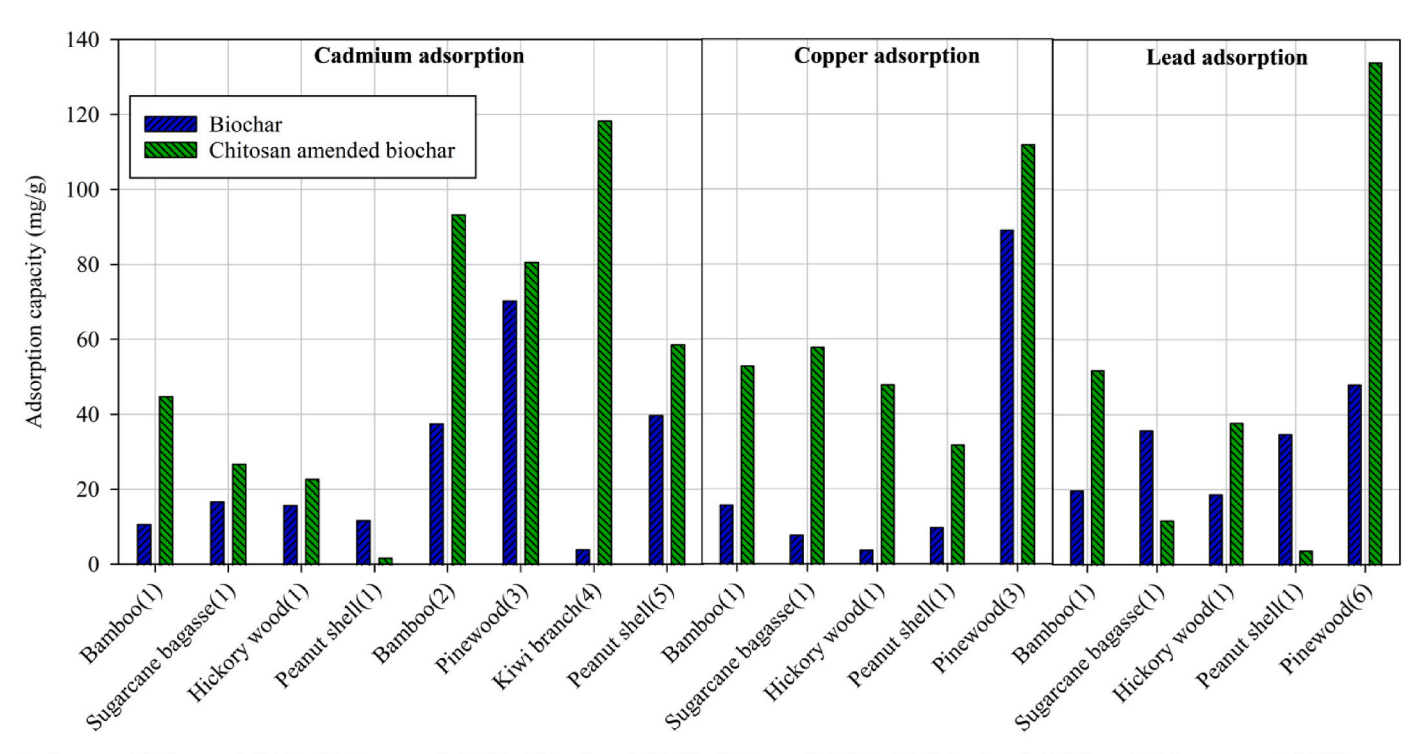
4.4.1. Heavy metal removal

Heavy metal adsorption by the CAB depends on the properties and

types of chitosan and biochar used for the composite synthesis and the heavy metal type. The adsorption capacities of the biochar and the corresponding CABs, as reported, are shown in Fig. 4, and the mechanisms involved, as presented in the literature, are discussed below.

Cadmium: Several studies reported a greater cadmium adsorption capacity for CAB than for biochar alone. CAB from bamboo biochar had a cadmium adsorption capacity of 45 mg/g compared to 11 mg/g for the biochar alone (Zhou et al., 2013). Another chitosan-bamboo biochar composite reported a maximum adsorption capacity of 37.74 mg/g for biochar alone and 93.46 mg/g for the composite (Huang et al., 2022). The Cd²⁺ adsorption capacity of a composite synthesized from sugarcane bagasse biochar increased from 17 mg/g for biochar alone to 27 mg/g for the composite. The adsorption capacity of a hickory wood biochar composite was reported to be 23 mg/g compared to 16 mg/g for biochar alone (Zhou et al., 2013). A composite synthesized from pine wood biochar (produced from gasification) also reportedly had an increase in the adsorption capacity of cadmium from 70.5 mg/g for biochar alone to 80.8 mg/g for the composite (Burk et al., 2020). The Cd²⁺adsorption capacity of a kiwi branch biochar composite was reported to increase from 4.24 mg/g for biochar alone to a maximum adsorption capacity of 118.43 mg/g for the composite (Tan et al., 2022). A peanut shell biochar composite had a decrease in adsorption capacity as reported from 12 mg/g for biochar alone to 2 mg/g for the composite (Zhou et al., 2013). Conversely, a peanut shell biochar prepared using a different method reportedly increased in capacity from 40 mg/g for biochar alone to 58.82 mg/g for the composite (Shabani et al., 2019).

The dominant interaction mechanism of cadmium ion (Cd²⁺)



References: (1) Zhou et al. (2013), (2) Huang et al. (2022), (3) Burk et al. (2020), (4) Tan et al. (2022), (5) Shabani et al. (2020), and (6) Dewage et al. (2018)

Fig. 4. Heavy metal adsorption capacities of biochar and corresponding chitosan-biochar composites as reported in the reviewed studies.

adsorption on CAB has been attributed to electrostatic interactions (Zhou et al., 2013; Huang et al., 2022). The positively charged Cd²⁺ ions are thought to adsorb to the electron-rich amine and oxygen containing groups on the CAB surface. Cadmium ions are also thought to exchange ion with metals such as Na⁺, Mg²⁺, K⁺ on the composite surface. The contaminant heavy metal ion replaces ions from the surface of the composite depending on the affinity towards the metal (Shabani et al., 2019; Tan et al., 2022). Other mechanisms have been attributed to cadmium ion removal, including physical adsorption on the CAB surface (Zhou et al., 2013; Huang et al., 2022), interactions with the amine and hydroxyl groups on the chitosan molecules and oxygen-containing functional groups on the biochar surfaces, Cd⁺² complexation on the CAB surface (kiwi branch biochar) and precipitation of cadmium in the form of cadmium carbonate in the presence of calcium carbonate available on the CAB surface (Tan et al., 2022), metal ion chelation, and covalent bonding with the chitosan polymer molecule (Zhou et al., 2013).

Most studies found in the literature reported an increase in the cadmium adsorption capacities for CAB when compared to biochar alone. However, the decrease in the adsorption capacities in some studies was explained by the significant decrease in the surface area and pore volume (Zhou et al., 2013).

Copper: Copper removal from aqueous solution was reported in different studies using CAB composites obtained from sugarcane bagasse, bamboo, hickory wood, peanut hull, sludge-based biochar, and gasified pine wood biochar. As reported by Zhou et al. (2013), the changes in adsorption capacities for different types of CABs when compared to biochar alone are as follows: bamboo biochar composite adsorption capacity increased significantly from 16 mg/g for biochar alone to 53 mg/g for the composite; adsorption capacity of sugarcane bagasse biochar composite increased from 8 mg/g for biochar alone to 58 mg/g for the composite; adsorption capacity of hickory wood biochar composite was 48 mg/g compared to 4 mg/g for biochar alone; and peanut hull biochar composite adsorption capacity was 32 mg/g compared to 10 mg/g for biochar alone. Sludge-based biochar composite was reported to have an adsorption rate of 97.5% at 0.5 g/L of

adsorbent dosage and a contaminant concentration of 0.06185 mg/L, higher than that of biochar alone (Song et al., 2021). Gasified pine wood biochar when combined with chitosan had an increase in the adsorption capacity from 89.2 mg/g for biochar alone to 112 mg/g for the composite (Burk et al., 2020). Adsorption mechanisms involved in the removal of copper, as reported or hypothesized in these studies are as follows: intraparticle diffusion when metal ions become trapped in the pores of the composite; chelation of copper metal ions with the chitosan of CAB; π - π interactions with overlapping of electron orbitals of the metal and the amine group from the chitosan; hydrogen bonding or ion-dipole interactions with amine and oxygen-containing groups of the CAB; hydrophobic interactions with the amine group and oxygen-containing groups along with surface adsorption and electrostatic interactions.

Lead: Different studies reported increased lead adsorption capacities with CAB when compared to biochar alone. However, sugarcane bagasse biochar composite and peanut hull biochar composite were reported to have a decrease in adsorption capacity for lead adsorption. The reduction for sugarcane bagasse biochar composite was reported to be from 36 mg/g for biochar alone to 19 mg/g for the composite and from 35 mg/g for biochar alone to 4 mg/g for the composite. The reduction was attributed to decreased composite surface area and pore volume when compared to biochar alone. The CAB composites of bamboo biochar, hickory wood biochar, sludge-based biochar, and pine wood biochar were reported to increase adsorption capacity compared to their corresponding biochar. For bamboo biochar composite, the increase was reported to be from 20 mg/g to 52 mg/g; for hickory wood biochar composite the increase was from 19 mg/g to 38 mg/g (Zhou et al., 2013), the adsorption rate of sludge-based biochar composite for lead was reported to be 94.3%, higher than that of biochar alone (Song et al., 2021). The maximum adsorption capacity of pine wood biochar was 48.2 mg/g which increased to 134 mg/g for the CAB (Dewage et al., 2018). Zhou et al. (2013), performed FTIR studies of bamboo biochar composite post-adsorption tests with lead, which were utilized to investigate the possible sorption mechanisms. The predominant mechanism responsible was reported to be electrostatic interactions of the

positively charged metal ions with the electron-rich amine group and oxygen containing hydroxyl groups. Chelation of the metal ions, intraparticle diffusion into the pores of the CAB, π - π interactions, and hydrogen bonding are some of the other mechanisms reported or hypothesized to have played a role in lead removal. The increase in the adsorption capacity of CAB composites compared to biochar alone in these studies was attributed to adding amine groups from chitosan.

Chromium and Selenium: A sludge-based biochar composite was investigated for the adsorption of chromium and selenium from oil sand process water (OSPW) (Song et al., 2021). The OSPW contained initial concentrations of 0.02914 mg/L and 0.008 mg/L of chromium and selenium, respectively. The OSPW was treated with 0.5 g/L of adsorbent. The adsorption rates were reported as 83.9% for chromium and 87.9% for selenium, higher than the adsorption rates for the biochar alone. Based on X-ray Photoelectron Spectroscopy (XPS) studies on the composite after adsorption, Song et al. (2021) concluded that oxygen-containing functional groups and the amine groups predominantly influenced the composite adsorption rates through electrostatic interactions with electron-rich amine groups and hydroxyl groups. In addition to the electrostatic interactions, π - π interactions, hydrogen bonding, and hydrophobic interactions between metals and oxygen-containing functional groups were also reported to affect the adsorption of metals onto the CAB (Song et al., 2021; Afzal et al., 2018). Some of these mechanisms involved in removing heavy metals are illustrated in Fig. 5.

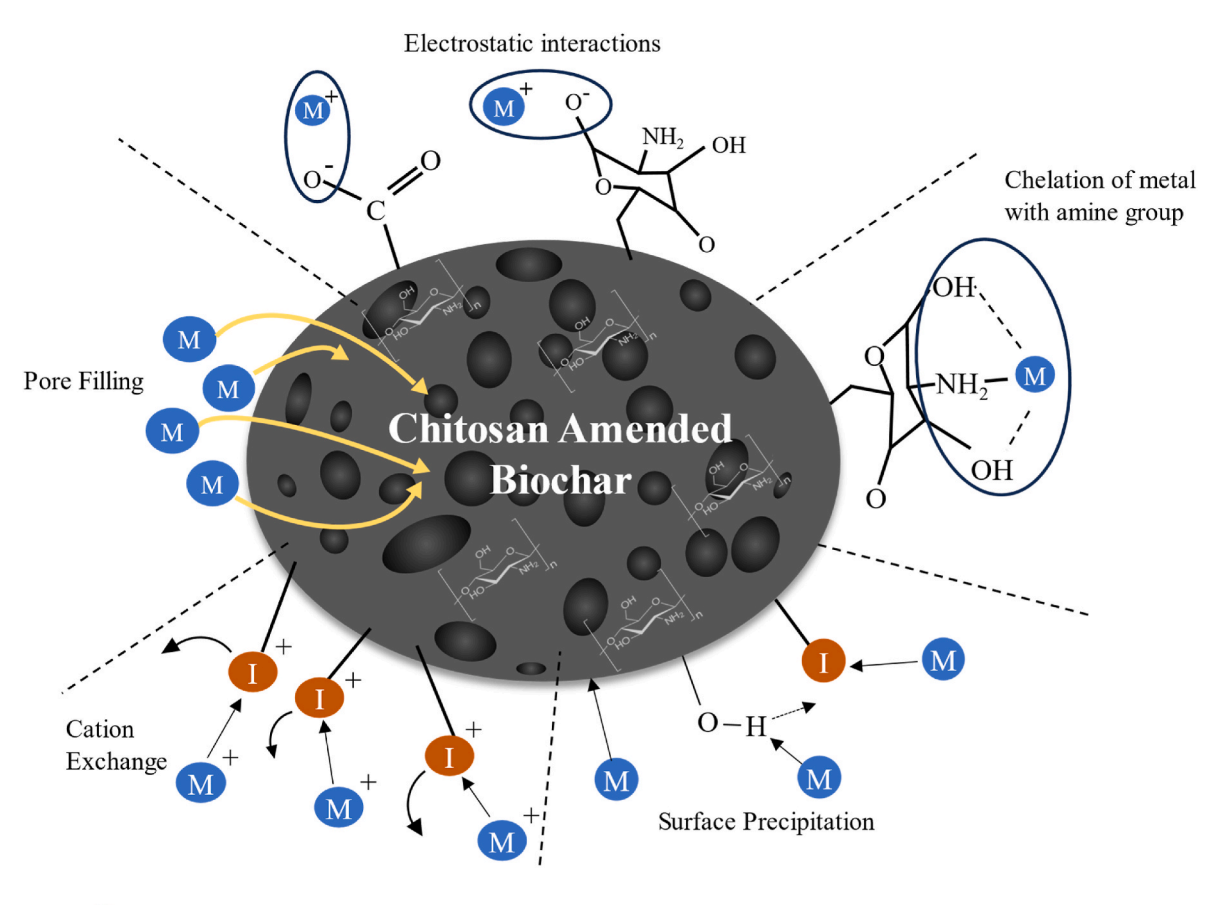
4.4.2. Drugs, dyes, and organics

Drugs: CAB produced from pomelo peel was used for adsorption of

the drug ciprofloxacin (Afzal et al., 2018). The adsorption capacity of the composite produced was reported to be 36.72~mg/g when 1 g of the composite was exposed to a contaminant concentration of 50~mg/L, and a total volume of 200~mL. The adsorption capacity of pure biochar was reported as 3.31~mg/g under similar conditions. The mechanisms responsible for removal were reported as ciprofloxacin forming hydrogen bonds with the amine groups of chitosan and the hydroxyl groups on the biochar surface and covalent interactions between ciprofloxacin and the amine groups of chitosan. FTIR studies on the composite after adsorption found peaks associated with the bonds between carbon and nitrogen of the composite and the antibiotic.

<u>Dyes:</u> CAB produced from raw rice husk biochar was used to remove methyl orange, an organic dye, from an aqueous solution (Loc et al., 2022). Methyl orange is anionic, and thus its adsorption is pH-dependent with higher adsorption at acidic pH. Protonation of the composite amine and hydroxyl groups in acidic pH has a higher affinity to the negatively charged methyl orange molecules. The adsorption capacity increased from 31.63 mg/g for the biochar alone to 38.75 mg/g for the composite (Langmuir model). Complexation of the dye on the composite surface, along with electrostatic interactions between the negatively charged methyl orange molecule sites and the protonated groups on the biochar surface and chitosan were the reported mechanisms involved in the adsorption of methyl orange dye (Loc et al., 2022).

Roy et al. (2022) synthesized CAB from *Moringa oleifera* seed biochar to investigate the adsorption of cationic methylene blue dye. The biochar alone had an adsorption capacity of 78 mg/g which increased to 180 mg/g for the composite. Pore diffusion was the dominant mechanism attributed to the adsorption of biochar alone. However, the surface



- Exchangeable metal ion Na +, K+, Ca²⁺
- M Contaminant metal ion

Fig. 5. Heavy metal adsorption mechanisms with chitosan-biochar composites, as reported in the reviewed studies.

area and the pore volume of the composite were found to be lower than that of the pure biochar. Hence, the contribution from pore diffusion was lower in the composite case. The predominant adsorption mechanisms for the composite were likely electrostatic interactions between the electron-dense amine groups of chitosan with the cationic dye as well as hydrogen bonding between the oxygen-containing functional groups on the composite surface and the nitrogen in the dye.

Other Organic Contaminants: CAB synthesized from wheat straw biochar was investigated for removing dissolved organic matter (DOM) from biotreated cooking wastewater (Shi et al., 2020). The removal efficiency for the composite (52%) was higher than that of biochar alone (12%). XPS studies of the composite after adsorption indicated that the removal mechanisms involved were electrostatic interactions between the negatively charged organic molecules with the amine groups from chitosan and hydrogen bonds with the hydroxyl groups of the biochar and nitrogen of the amine group of the chitosan. The measured composite pore volume and surface area decreased after the adsorption tests indicating the entry of the DOM into the pores of the composite. Acid-base reactions with the acidic groups of the DOM and the protonated amine groups of chitosan were also reported to contribute to the DOM removal (Shi et al., 2020).

5. Chitosan-bentonite-biochar composites

5.1. Synthesis

Chitosan-biochar-clay composites are a less studied area as only two studies focusing on the composite synthesized from all three materials were found in the literature (Arabyarmohammadi et al., 2018a; b). These studies produced the biochar from Mazandaran wood and paper plant bark chips by pyrolysis at 600 $^{\circ}$ C for 2 h under nitrogen conditions with a heating rate of 10 $^{\circ}$ C/min. The resulting biochar was then rinsed with deuterium-depleted water and oven-dried at 80 $^{\circ}$ C.

The composite was then synthesized according to the following steps. (1) A chitosan solution was prepared by dissolving 5 g of commercially obtained chitosan powder in 250 mL acetic acid (2%). (2) A nano clay suspension with 5% clay content in 10 ml acetic acid (2%) was prepared. (3) The chitosan solution was gradually added into the nano clay suspension and stirred for 24 h (4) 5 g of biochar was added to the mixture and stirred for 30 min (5) The biochar/chitosan/clay suspension was then added dropwise into 1000 ml NaOH solution (1.2%) and kept in solution for 12 h (6) The composite solids were filtered out and washed with deuterium-depleted water to remove any excess NaOH, followed by oven drying at 70 °C (Arabyarmohammadi et al., 2018a; b).

5.2. Interactions

FTIR was used to identify functional groups in the CBBC (Arabyar-mohammadi et al., 2018a; b). When compared with the pure chitosan, a shift in the peak that corresponds to N–H was observed. This indicates the interaction of the negatively charged clay surface with the protonated amine groups of chitosan. The bands corresponding to C–H groups also shifted, indicating the interaction between the chitosan and clay mineral surfaces.

5.3. Properties

FTIR analysis on the CBBC indicated the stretching of O–H, N–H, and C–H bands due to interactions between chitosan and the negatively charged clay particles. XRD and TEM studies investigated the mode of engagement between the clay and the chitosan molecules. XRD of the clay had a reflection at $2\theta=8.88^\circ$, whereas the composite had none. This difference was hypothesized to indicate the intercalation and exfoliation of clay into the chitosan matrix. The TEM images of the composites reportedly confirmed this. PZC of the CBBC affects its net surface charge and thus affects the adsorption capacities and

mechanisms of contaminants. The CBBC's PZC (pH_{zpc}) was reported as pH 6.8, indicating a negative net surface charge in the neutral pH, indicating possible electrostatic interactions with positively charged heavy metal contaminants.

5.4. Contaminant removal – capacities and mechanisms

Arabyarmohammadi et al. (2018a,b) investigated their CBBC to remove heavy metals copper, zinc, and lead. The adsorption tests were conducted at 12 initial concentrations for each contaminant and at three different temperatures (25 °C, 40 °C, 60 °C). The maximum adsorption capacities were found to be 121.5, 134.6, and 336 mg/g for copper, zinc, and lead, respectively, at 25 °C. The mechanisms involved in the removal were hypothesized to be chemical reactions between the functional groups of the CBBC and the metals, and physical diffusion into the composite pores. FTIR analysis on the composite after the adsorption tests indicated bonding between the amine groups of chitosan and the metals. Multi-element adsorption tests were conducted, and the composite had a higher affinity for lead than copper and zinc. Elemental mapping results post-adsorption agreed with a denser map for lead (Arabyarmohammadi et al., 2018a). The study also compared the composite adsorption capacity of the selected three metals with biochar alone and chitosan alone from other studies by different researchers. The composite had an over 10-fold increase in copper and zinc adsorption capacity when compared to biochar alone (Chen et al., 2011) and more than double the capacity when compared with chitosan alone (Shobanardakani et al., 2014).

Arabyarmohammadi et al. (2018)b conducted column tests to investigate the leachability of those metals from soil amended with the CBBC composite. The reduction in leaching of lead, copper, and zinc was reported as 100%, 100%, and 52.29%, respectively.

6. Future Research directions

Several studies demonstrate the efficiency of chitosan-based composites with bentonite (CBC) and biochar (CAB) for the removal of diverse contaminants. However, chitosan may have limitations regarding mechanical strength and permeability that may limit its applications in barrier systems. Combining chitosan with other materials, such as biochar and bentonite, might overcome these performance limitations. However, very few studies on CBBC for contaminant removal applications are available. Additionally, the performance of these composites under mixed contamination conditions has received limited attention.

Furthermore, chitosan and biochar are derived from waste materials and thus possess inherent uncertainties in their material properties and adsorption capacities. Hence, carefully considering these uncertainties is crucial before employing these materials in containment barriers. The future prospects for utilizing chitosan-based composites, specifically CBC, CAB, and CBBC, in barrier systems depend on addressing these limitations through comprehensive studies. These studies should include investigations into different sources of materials and their efficacy against various contaminants, along with pilot-scale and field-scale assessments, and finally the development of effective composite materials.

Additionally, cost assessments specific to the proposed area are needed to understand the economic viability of the proposed barrier system made with these materials. Furthermore, a comprehensive resilience and sustainability assessment can help in the critical evaluation of a potential barrier system resulting from these materials. Our ongoing research studies aim to address these limitations and develop the most effective chitosan-based composites for mixed contaminant applications.

While there is variability in chitosan, bentonite, and biochar properties, these uncertainties can be minimized by creating engineered composites. These novel composite materials can be proportioned to remain cost-effective and applied to surface and groundwaters

containing various contaminants.

7. Summary

Numerous methods have been explored to address subsurface contamination through barrier systems made from various materials. The contaminants of concern are diverse and pose a unique challenge for mitigation. Bentonite is commonly used in barrier systems due to its low permeability but is limited in its adsorption capacities and compatibility with contaminants. Chitosan, on the other hand, has amine and hydroxyl groups along the polymer chain that can interact with a wide range of contaminants through various mechanisms but is limited by its undesirable physical properties and biodegradability. A composite synthesized from chitosan and bentonite potentially combines the desired properties of both materials, enhancing contaminant removal. Similarly, biochar, with its high porosity and specific surface area when combined with chitosan in composite form, is used to remove organics, dyes, heavy metals, drugs, etc.

Different procedures have been employed to prepare chitosan-based composites of bentonite and biochar, which are used to remove various contaminants. The adsorption capacities of these composites depend on the surface chemistry and the mechanisms involved in the contaminant removal. Given the wide range of contaminants in the surface water runoffs, investigating the possible adsorption mechanisms is crucial. The surface chemistry and properties of the composites heavily depend on the properties of the raw materials used and their interactions. Hence, a detailed analysis of synthesis procedures used in preparing chitosan bentonite composites (CBCs), and chitosan biochar composites (CABs) provides an understanding of the properties of the composites. These procedures aid in understanding the changes in properties associated with the preparation conditions. Furthermore, comparing FTIR, XRD, and SEM analyses of the composites with those of pure materials offers insights into the interactions among the composite components.

The adsorption capacities of the composites CBCs and CABs against contaminants like heavy metals, organics, dyes, drugs, and water turbidity, particularly in groundwater treatment, are identified to be an improvement over the pure materials from the literature available.

Chitosan bentonite biochar composites (CBBCs), on the other hand, have received very little attention, with only two studies thus far focusing on their contaminant removal capabilities. The synthesis procedure of CBBC mirrors that of CBC, with biochar added as an extra step. The FTIR analysis of the composite and the pure materials indicate clay-chitosan interaction. The composite, tested for heavy metal adsorption, reveals the potential of CBBCs in this application. Upon comparison with similar studies on pure materials, the adsorption capacities of the composite reportedly show enhanced capacity.

In all, this review discusses various bentonite and biochar-based composites of chitosan, their contaminant removal capacities against a wide range of contaminants and the mechanisms involved in the process. Furthermore, this study presents the potential of the composite synthesized from all three materials, chitosan, bentonite, and biochar, for enhanced removal of diverse contaminants. Finally, this study discusses the challenges associated with the uncertainties with the material properties of chitosan and biochar and future research directions in the synthesis and use of CBBCs in contaminant removal.

CRediT authorship contribution statement

Banuchandra Nagaraja: Writing – review & editing, Writing – original draft, Methodology, Investigation, Formal analysis, Conceptualization. Jagadeesh Kumar Janga: Writing – original draft, Methodology, Investigation, Formal analysis, Conceptualization. Sadam Hossain: Writing – original draft, Methodology, Investigation, Formal analysis, Conceptualization. Gaurav Verma: Writing – original draft, Methodology, Investigation, Conceptualization. Angelica M. Palomino: Writing – review & editing, Writing – original draft, Supervision,

Resources, Project administration, Methodology, Investigation, Funding acquisition, Conceptualization. **Krishna R. Reddy:** Writing – review & editing, Writing – original draft, Supervision, Resources, Project administration, Methodology, Investigation, Funding acquisition, Formal analysis, Conceptualization.

Declaration of competing interest

The authors declare that they have no known competing financial interests or personal relationships that could have appeared to influence the work reported in this paper.

Data availability

Data will be made available on request.

Acknowledgments

This research is part of a comprehensive project titled "Development of Novel Chitosan-Biochar-Bentonite Composite Barrier Resilient to Changing Climate: Synthesis, Characterization, and Containment Mechanisms" funded by the National Science Foundation (CMMI# 2225303), which is gratefully acknowledged. Any opinions, findings, conclusions, and recommendations expressed in this material are those of the authors and do not necessarily reflect the views of the NSF.

References

- Afzal, M.Z., Sun, X.F., Liu, J., Song, C., Wang, S.G., Javed, A., 2018. Enhancement of ciprofloxacin sorption on chitosan/biochar hydrogel beads. Sci. Total Environ. 639, 560, 560
- Aizat, M.A., Aziz, F., 2019. Chitosan nanocomposite application in wastewater treatments. In: Nanotechnology in Water and Wastewater Treatment. Elsevier, pp. 243–265.
- Aliabadi, M., Irani, M., Ismaeili, J., Najafzadeh, S., 2014. Design and evaluation of chitosan/hydroxyapatite composite nanofiber membrane for the removal of heavy metal ions from aqueous solution. J. Taiwan Inst. Chem. Eng. 45 (2), 518–526.
- Arabyarmohammadi, H., Darban, A.K., Abdollahy, M., Yong, R., Ayati, B., Zirakjou, A., van der Zee, S.E., 2018a. Utilization of a novel chitosan/clay/biochar nanobiocomposite for immobilization of heavy metals in acid soil environment. J. Polym. Environ. 26, 2107–2119.
- Arabyarmohammadi, H., Darban, A.K., van der Zee, S.E., Abdollahy, M., Ayati, B., 2018b. Fractionation and leaching of heavy metals in soils amended with a new biochar nanocomposite. Environ. Sci. Pollut. Control Ser. 25, 6826–6837.
- Ardila, N., Daigle, F., Heuzey, M.C., Ajji, A., 2017. Antibacterial activity of neat chitosan powder and flakes. Molecules 22 (1), 100.
- Ashford, N.A., Hattis, D., Murray, A.E., 1977. Industrial Prospects for Chitin and Protein from Shellfish Wastes: a Report on the First Marine Industries Business Strategy Program Marine Industry Advisory Service.
- Bhatnagar, A., Sillanpää, M., 2009. Applications of chitin-and chitosan-derivatives for the detoxification of water and wastewater—a short review. Adv. Colloid Interface Sci. 152 (1–2), 26–38.
- Binaeian, E., Zadvarzi, S.B., Yuan, D., 2020. Anionic dye uptake via composite using chitosan-polyacrylamide hydrogel as matrix containing TiO2 nanoparticles; comprehensive adsorption studies. Int. J. Biol. Macromol. 162, 150–162.
- Biswas, S., Fatema, J., Debnath, T., Rashid, T.U., 2021. Chitosan–clay composites for wastewater treatment: a state-of-the-art review. ACS ES&T Water 1 (5), 1055–1085.
- Bleiman, N., Mishael, Y.G., 2010. Selenium removal from drinking water by adsorption to chitosan–clay composites and oxides: batch and columns tests. J. Hazard Mater. 183 (1–3), 590–595.
- Boddu, V.M., Abburi, K., Randolph, A.J., Smith, E.D., 2008. Removal of copper (II) and nickel (II) ions from aqueous solutions by a composite chitosan biosorbent. Separ. Sci. Technol. 43 (6), 1365–1381.
- Budnyak, T.M., Yanovska, E.S., Kichkiruk, O.Y., Sternik, D., Tertykh, V.A., 2016. Natural minerals coated by biopolymer chitosan: synthesis, physicochemical, and adsorption properties. Nanoscale Res. Lett. 11, 1–12.
- Burk, G.A., Herath, A., Crisler, G.B., Bridges, D., Patel, S., Pittman Jr, C.U., Mlsna, T., 2020. Cadmium and copper removal from aqueous solutions using chitosan-coated gasifier biochar. Front. Environ. Sci. 8, 541203.
- Calvo, P., Remunan-Lopez, C., Vila-Jato, J.L., Alonso, M.J., 1997. Novel hydrophilic chitosan-polyethylene oxide nanoparticles as protein carriers. J. Appl. Polym. Sci. 63 (1), 125–132.
- Celis, R., Adelino, M.A., Hermosín, M.C., Cornejo, J., 2012. Montmorillonite-chitosan bionanocomposites as adsorbents of the herbicide clopyralid in aqueous solution and soil/water suspensions. J. Hazard Mater. 209, 67–76.
- Cestari, A.R., Vieira, E.F., Dos Santos, A.G., Mota, J.A., De Almeida, V.P., 2004.

 Adsorption of anionic dyes on chitosan beads. 1. The influence of the chemical

- structures of dyes and temperature on the adsorption kinetics. J. Colloid Interface Sci. 280 (2), 380–386.
- Chen, X., Chen, G., Chen, L., Chen, Y., Lehmann, J., McBride, M.B., Hay, A.G., 2011. Adsorption of copper and zinc by biochars produced from pyrolysis of hardwood and corn straw in aqueous solution. Bioresour. Technol. 102 (19), 8877–8884.
- Cheng, J., Xie, S., Wang, S., Xue, Y., Jiang, L., Liu, L., 2017. Optimization of protein removal from soybean whey wastewater using chitosan ultrafiltration. J. Food Process. Eng. 40 (2), e12370.
- Cheng, H., Zhu, Q., Wang, A., Weng, M., Xing, Z., 2020. Composite of chitosan and bentonite cladding Fe–Al bimetal: effective removal of nitrate and by-products from wastewater. Environ. Res. 184, 109336.
- Chetri, J.K., Reddy, K.R., Green, S.J., 2022. Use of methanotrophically activated biochar in novel biogeochemical cover system for carbon sequestration: microbial characterization. Sci. Total Environ. 821, 153429.
- Chiou, M.S., Li, H.Y., 2003. Adsorption behavior of reactive dye in aqueous solution on chemical cross-linked chitosan beads. Chemosphere 50 (8), 1095–1105.
- Cohen, E., Poverenov, E., 2022. Hydrophilic chitosan derivatives: synthesis and applications. Chem.–Eur. J. 28 (67), e202202156.
- Crini, G., Badot, P.M., 2008. Application of chitosan, a natural aminopolysaccharide, for dye removal from aqueous solutions by adsorption processes using batch studies: a review of recent literature. Prog. Polym. Sci. 33 (4), 399–447.
- Dai, L., Lu, Q., Zhou, H., Shen, F., Liu, Z., Zhu, W., Huang, H., 2021. Tuning oxygenated functional groups on biochar for water pollution control: a critical review. J. Hazard Mater. 420, 126547.
- Darder, M., Colilla, M., Ruiz-Hitzky, E., 2003. Biopolymer clay nanocomposites based on chitosan intercalated in montmorillonite. Chem. Mater. 15 (20), 3774–3780.
- Davila-Rodriguez, J.L., Escobar-Barrios, V.A., Shirai, K., Rangel-Mendez, J.R., 2009. Synthesis of a chitin-based biocomposite for water treatment: optimization for fluoride removal. J. Fluor. Chem. 130 (8), 718–726.
- de Moraes, M.A., Cocenza, D.S., da Cruz Vasconcellos, F., Fraceto, L.F., Beppu, M.M., 2013. Chitosan and alginate biopolymer membranes for remediation of contaminated water with herbicides. J. Environ. Manag. 131, 222–227.
- Dehghani, M.H., Zarei, A., Mesdaghinia, A., Nabizadeh, R., Alimohammadi, M., Afsharnia, M., McKay, G., 2018. Production and application of a treated bentonite-chitosan composite for the efficient removal of humic acid from aqueous solution. Chem. Eng. Res. Des. 140, 102–115.
- Devi, N., Dutta, J., 2017. Preparation and characterization of chitosan-bentonite nanocomposite films for wound healing application. Int. J. Biol. Macromol. 104, 1897–1904.
- Dewage, N.B., Fowler, R.E., Pittman, C.U., Mohan, D., Mlsna, T., 2018. Lead (Pb 2+) sorptive removal using chitosan-modified biochar: batch and fixed-bed studies. RSC Adv. 8 (45), 25368–25377.
- Dotto, G.L., Moura, J.M.D., Cadaval, T.R.S., Pinto, L.A.D.A., 2013. Application of chitosan films for the removal of food dyes from aqueous solutions by adsorption. Chem. Eng. J. 214, 8–16.
- Dotto, G.L., Rodrigues, F.K., Tanabe, E.H., Fröhlich, R., Bertuol, D.A., Martins, T.R., Foletto, E.L., 2016. Development of chitosan/bentonite hybrid composite to remove hazardous anionic and cationic dyes from colored effluents. J. Environ. Chem. Eng. 4 (3), 3230–3239.
- El-Dib, F.I., Tawfik, F.M., Eshaq, G., Hefni, H.H.H., ElMetwally, A.E., 2016. Remediation of distilleries wastewater using chitosan immobilized Bentonite and Bentonite based organoclays. Int. J. Biol. Macromol. 86, 750–755.
- Foroutan, R., Peighambardoust, S.J., Mohammadi, R., Omidvar, M., Sorial, G.A., Ramavandi, B., 2020. Influence of chitosan and magnetic iron nanoparticles on chromium adsorption behavior of natural clay: adaptive neuro-fuzzy inference modeling. Int. J. Biol. Macromol. 151, 355–365.
- Gao, N., Du, W., Zhang, M., Ling, G., Zhang, P., 2022. Chitosan-modified biochar: preparation, modifications, mechanisms and applications. Int. J. Biol. Macromol. 209, 31–49.
- Geetha Devi, M., Dumaran, J.J., Feroz, S., 2012. Dairy wastewater treatment using low molecular weight crab shell chitosan. J. Inst. Eng.: Series E 93, 9–14.
- Gentili, A.R., Cubitto, M.A., Ferrero, M., Rodriguéz, M.S., 2006. Bioremediation of crude oil polluted seawater by a hydrocarbon-degrading bacterial strain immobilized on chitin and chitosan flakes. Int. Biodeterior. Biodegrad. 57 (4), 222–228.
- Guan, Y.L., Shao, L.E.I., Yao, K.D., 1996. A study on correlation between water state and swelling kinetics of chitosan-based hydrogels. J. Appl. Polym. Sci. 61 (13), 2325–2335
- Günister, E., Pestreli, D., Ünlü, C.H., Atıcı, O., Güngör, N., 2007. Synthesis and characterization of chitosan-MMT biocomposite systems. Carbohydr. Polym. 67 (3), 358–365.
- Guzman, J., Saucedo, I., Navarro, R., Revilla, J., Guibal, E., 2002. Vanadium interactions with chitosan: influence of polymer protonation and metal speciation. Langmuir 18 (5), 1567–1573.
- Hsien, T.Y., Rorrer, G.L., 1997. Heterogeneous cross-linking of chitosan gel beads: kinetics, modeling, and influence on cadmium ion adsorption capacity. Ind. Eng. Chem. Res. 36 (9), 3631–3638.
- Hu Chao, H.C., Deng YouJun, D.Y., Hu HongQing, H.H., Duan YuHang, D.Y., Zhai Kun, Z. K., 2016. Adsorption and Intercalation of Low and Medium Molar Mass Chitosans On/in the Sodium Montmorillonite.
- Huang, A., Bai, W., Yang, S., Wang, Z., Wu, N., Zhang, Y., et al., 2022. Adsorption characteristics of chitosan-modified bamboo biochar in Cd (II) contaminated water. J. Chem. 2022, 1–10.
- IPCC 2021. Masson-Delmotte V et al., 2021. Climate change 2021: the physical science basis. Contribution of working group I to the sixth assessment report of the intergovernmental panel on climate change, 2(1), 2391.

Jia, J., Liu, Y., Sun, S., 2021. Preparation and characterization of chitosan/bentonite composites for Cr (VI) removal from aqueous solutions. Adsorpt. Sci. Technol. 2021, 1 15

- Jimtaisong, A., Sarakonsri, T., 2019. Chitosan intercalated bentonite as natural adsorbent matrix for water-soluble sappanwood dye. Int. J. Biol. Macromol. 129, 737–743.
- Jóźwiak, T., Filipkowska, U., Rodziewicz, J., Nowosad, E., 2013. Effect of cross-linking with glutaraldehyde on adsorption capacity of chitosan beads. Progress on Chemistry and Application of Chitin and its Derivatives 18 (18), 35–47.
- Koutsopoulou, E., Koutselas, I., Christidis, G.E., Papagiannopoulos, A., Marantos, I., 2020. Effect of layer charge and charge distribution on the formation of chitosansmectite bionanocomposites. Appl. Clay Sci. 190, 105583.
- Krupadam, R.J., Sridevi, P., Sakunthala, S., 2011. Removal of endocrine disrupting chemicals from contaminated industrial groundwater using chitin as a biosorbent. J. Chem. Technol. Biotechnol. 86 (3), 367–374.
- Kumar, M.N.R., 2000. A review of chitin and chitosan applications. React. Funct. Polym. 46 (1), 1–27.
- Kumar, A., Kumar, D., George, N., Sharma, P., Gupta, N., 2018. A process for complete biodegradation of shrimp waste by a novel marine isolate Paenibacillus sp. AD with simultaneous production of chitinase and chitin oligosaccharides. Int. J. Biol. Macromol. 109, 263–272.
- Kumararaja, P., Manjaiah, K.M., Datta, S.C., Ahammed Shabeer, T.P., Sarkar, B., 2018. Chitosan-g-poly (acrylic acid)-bentonite composite: a potential immobilizing agent of heavy metals in soil. Cellulose 25, 3985–3999.
- Kurita, K., 2001. Controlled functionalization of the polysaccharide chitin. Prog. Polym. Sci. 26 (9), 1921–1971.
- Kwok, K.C., Lee, V.K., Gerente, C., McKay, G., 2009. Novel model development for sorption of arsenate on chitosan. Chem. Eng. J. 151 (1–3), 122–133.
- Kwok, K.C., Koong, L.F., Chen, G., McKay, G., 2014. Mechanism of arsenic removal using chitosan and nanochitosan. J. Colloid Interface Sci. 416, 1–10.
- Li, B., Elango, J., Wu, W., 2020. Recent advancement of molecular structure and biomaterial function of chitosan from marine organisms for pharmaceutical and nutraceutical application. Appl. Sci. 10 (14), 4719.
- Liakos, E.V., Lazaridou, M., Michailidou, G., Koumentakou, I., Lambropoulou, D.A., Bikiaris, D.N., Kyzas, G.Z., 2021. Chitosan adsorbent derivatives for pharmaceuticals removal from effluents: a review. Macromolecules (Washington, DC, U. S.) 1 (2), 130–154.
- Liu, Q., Yang, B., Zhang, L., Huang, R., 2015. Adsorption of an anionic azo dye by crosslinked chitosan/bentonite composite. Int. J. Biol. Macromol. 72, 1129–1135.
- Liu, Y., Jia, J., Zhang, H., Sun, S., 2022. Enhanced Cr (VI) stabilization in soil by chitosan/bentonite composites. Ecotoxicol. Environ. Saf. 238, 113573.
- Loc, N.X., Tuyen, P.T.T., Mai, L.C., Phuong, D.T.M., 2022. Chitosan-modified biochar and unmodified biochar for methyl orange: adsorption characteristics and mechanism exploration. Toxics 10 (9), 500.
- Ma, Z., Du, W., Yan, Z., Chen, X., Wang, Y., Mao, Z., 2021. Removal of phloridzin by chitosan-modified biochar prepared from apple branches. Anal. Lett. 54 (5), 903–918.
- Manyatshe, A., Cele, Z.E., Balogun, M.O., Nkambule, T.T., Msagati, T.A., 2022. Chitosan modified sugarcane bagasse biochar for the adsorption of inorganic phosphate ions from aqueous solution. J. Environ. Chem. Eng. 10 (5), 108243.
- Moghimi, A., 2014. Separation and extraction of Co (II) using magnetic chitosan nanoparticles grafted with β -cyclodextrin and determination by FAAS. Russ. J. Phys. Chem. A 88, 2157–2164.
- Moret, A., Rubio, J., 2003. Sulphate and molybdate ions uptake by chitin-based shrimp shells. Miner. Eng. 16 (8), 715–722.
- Moussout, H., Ahlafi, H., Aazza, M., El Akili, C., 2018. Performances of local chitosan and its nanocomposite 5% Bentonite/Chitosan in the removal of chromium ions (Cr (VI)) from wastewater. Int. J. Biol. Macromol. 108, 1063–1073.
- Muliwa, A.M., Leswifi, T.Y., Maity, A., Ochieng, A., Onyango, M.S., 2018. Fixed-bed operation for manganese removal from water using chitosan/bentonite/MnO composite beads. Environ. Sci. Pollut. Control Ser. 25, 18081–18095.
- Muzzarelli, R.A., 1983. Chitin and its derivatives: new trends of applied research. Carbohydr. Polym. 3 (1), 53–75.
- Muzzarrelli, R.A.A., 1977. Chitin. Oxford Pergamon press, New York 309p.
- Nagarpita, M.V., Roy, P., Shruthi, S.B., Sailaja, R.R.N., 2017. Synthesis and swelling characteristics of chitosan and CMC grafted sodium acrylate-co-acrylamide using modified nanoclay and examining its efficacy for removal of dyes. Int. J. Biol. Macromol. 102, 1226–1240.
- Natural Resource Defense Council (NRDC), 2021. Flooding and Climate Change: Everything You Need to Know.
- Nesic, A.R., Velickovic, S.J., Antonovic, D.G., 2012. Characterization of chitosan/montmorillonite membranes as adsorbents for Bezactiv Orange V-3R dye. J. Hazard Mater. 209, 256–263.
- Ngulube, T., Gumbo, J.R., Masindi, V., Maity, A., 2017. An update on synthetic dyes adsorption onto clay based minerals: a state-of-art review. J. Environ. Manag. 191, 35–57.
- Oni, B.A., Oziegbe, O., Olawole, O.O., 2019. Significance of biochar application to the environment and economy. Ann. Agric. Sci. (Cairo) 64 (2), 222–236.
- Pal, P., Pal, A., Nakashima, K., Yadav, B.K., 2021. Applications of chitosan in environmental remediation: a review. Chemosphere 266, 128934.
- Palansooriya, K.N., Kim, S., Igalavithana, A.D., Hashimoto, Y., Choi, Y.E., Mukhopadhyay, R., et al., 2021. Fe (III) loaded chitosan-biochar composite fibers for the removal of phosphate from water. J. Hazard Mater. 415, 125464.
- Pan, J.R., Huang, C., Chen, S., Chung, Y.C., 1999. Evaluation of a modified chitosan biopolymer for coagulation of colloidal particles. Colloids Surf. A Physicochem. Eng. Asp. 147 (3), 359–364.

- Peniche-Covas, C., Alvarez, L.W., Argüelles-Monal, W., 1992. The adsorption of mercuric ions by chitosan. J. Appl. Polym. Sci. 46 (7), 1147–1150.
- Pereira, F.A., Sousa, K.S., Cavalcanti, G.R., França, D.B., Queiroga, L.N., Santos, I.M., et al., 2017. Green biosorbents based on chitosan-montmorillonite beads for anionic dye removal. J. Environ. Chem. Eng. 5 (4), 3309–3318.
- Pitt, R., Field, R., Lalor, M., Brown, M., 1995. Urban stormwater toxic pollutants: assessment, sources, and treatability. Water Environ. Res. 67 (3), 260–275.
- Qiu, B., Tao, X., Wang, H., Li, W., Ding, X., Chu, H., 2021. Biochar as a low-cost adsorbent for aqueous heavy metal removal: a review. J. Anal. Appl. Pyrol. 155, 105081.
- Ramachandran Nair, K.G., Madhavan, P., 1984. Chitosan for Removal of Mercury from Water
- Reddy, K.R., Xie, T., Dastgheibi, S., 2014. Evaluation of biochar as a potential filter media for the removal of mixed contaminants from urban storm water runoff. J. Environ. Eng. 140 (12), 04014043.
- Reddy, K.R., Cameselle, C., Adams, J.A., 2019. Sustainable Engineering: Drivers, Metrics, Tools, and Applications. John Wiley & Sons.
- Reiad, N.A., Salam, O.E.A., Abadir, E.F., Harraz, F.A., 2012. Adsorptive removal of iron and manganese ions from aqueous solutions with microporous chitosan/ polyethylene glycol blend membrane. J. Environ. Sci. 24 (8), 1425–1432.
- Rinaudo, M., 2006. Chitin and chitosan: properties and applications. Prog. Polym. Sci. 31 (7), 603–632.
- Robinson-Lora, M.A., Brennan, R.A., 2009. Efficient metal removal and neutralization of acid mine drainage by crab-shell chitin under batch and continuous-flow conditions. Bioresour. Technol. 100 (21), 5063–5071.
- Robinson-Lora, M.A., Brennan, R.A., 2010. Chitin complex for the remediation of mine impacted water: geochemistry of metal removal and comparison with other common substrates. Appl. Geochem. 25 (3), 336–344.
- Rorrer, G.L., Hsien, T.Y., Way, J.D., 1993. Synthesis of porous-magnetic chitosan beads for removal of cadmium ions from wastewater. Ind. Eng. Chem. Res. 32 (9), 2170–2178.
- Rowe, R.K., 2001. Barrier systems. In: Rowe, R.K. (Ed.), Geotechnical and Geoenvironmental Engineering Handbook. Springer, Boston, MA.
- Roy, H., Islam, M.S., Arifin, M.T., Firoz, S.H., 2022. Synthesis, characterization and sorption properties of biochar, chitosan and ZnO-based binary composites towards a cationic dve. Sustainability 14 (21), 14571.
- Sabnis, S., Block, L.H., 1997. Improved infrared spectroscopic method for the analysis of degree of N-deacetylation of chitosan. Polym. Bull. 39, 67–71.
- Sadeghi-Kiakhani, M., Arami, M., Gharanjig, K., 2013. Preparation of chitosan-ethyl acrylate as a biopolymer adsorbent for basic dyes removal from colored solutions. J. Environ. Chem. Eng. 1 (3), 406–415.
- Sellaoui, L., Soetaredjo, F.E., Ismadji, S., Bonilla-Petriciolet, A., Belver, C., Bedia, J., et al., 2018. Insights on the statistical physics modeling of the adsorption of Cd2+ and Pb2+ ions on bentonite-chitosan composite in single and binary systems. Chem. Eng. J. 354, 569–576.
- Şenol, Z.M., Şimşek, S., 2022. Insights into effective adsorption of lead ions from aqueous solutions by using chitosan-bentonite composite beads. J. Polym. Environ. 30 (9), 3677–3687
- Shabani, H., Delavar, M.A., Taghavi Fardood, S., 2019. Sorption of cd (II) ions by chitosan modified peanut shell biochar from aqueous solution. Advances in Environmental Technology 5 (4), 203–211.
- Shi, Y., Hu, H., Ren, H., 2020. Dissolved organic matter (DOM) removal from biotreated coking wastewater by chitosan-modified biochar: adsorption fractions and mechanisms. Bioresour. Technol. 297, 122281.
- Sobhanardakani, S., Zandipak, R., Parvizimosaed, H., Javanshir Khoei, A., Moslemi, M., Tahergorabi, M., et al., 2014. Efficiency of chitosan for the removal of Pb (II), Fe (II) and Cu (II) ions from aqueous solutions. Iranian Journal of Toxicology 8 (26), 1145–1151
- Song, J., Messele, S.A., Meng, L., Huang, Z., El-Din, M.G., 2021. Adsorption of metals from oil sands process water (OSPW) under natural pH by sludge-based Biochar/ Chitosan composite. Water Res. 194, 116930.
- Sudha, P.N., 2010. 39 chitin/chitosan and derivatives for wastewater treatment. Chitin. Chitosan, Oligosaccharides and Their Derivatives 561.
- Sudha, P.N., Sangeetha, K., Gomathi, T., 2017. Introduction to marine biopolymers. In: Industrial Applications of Marine Biopolymers. CRC Press, pp. 3–18.
- Syafalni, S., Abustan, I., Zakaria, S.N.F., Zawawi, M.H., Rahim, R.A., 2012. Raw water treatment using bentonite-chitosan as a coagulant. Water Sci. Technol. Water Supply 12 (4), 480–488.
- Synowiecki, J., Al-Khateeb, N.A., 2003. Production, Properties, and Some New Applications of Chitin and its Derivatives.

- Tan, K.B., Vakili, M., Horri, B.A., Poh, P.E., Abdullah, A.Z., Salamatinia, B., 2015. Adsorption of dyes by nanomaterials: recent developments and adsorption mechanisms. Separ. Purif. Technol. 150, 229–242.
- Tan, Y., Wan, X., Ni, X., Wang, L., Zhou, T., Sun, H., et al., 2022. Efficient removal of Cd (II) from aqueous solution by chitosan modified kiwi branch biochar. Chemosphere 289, 133251.
- Topcu, C., Caglar, B., Onder, A., Coldur, F., Caglar, S., Guner, E.K., et al., 2018. Structural characterization of chitosan-smectite nanocomposite and its application in the development of a novel potentiometric monohydrogen phosphate-selective sensor. Mater. Res. Bull. 98, 288–299.
- Upadhyay, U., Sreedhar, I., Singh, S.A., Patel, C.M., Anitha, K.L., 2021. Recent advances in heavy metal removal by chitosan based adsorbents. Carbohydr. Polym. 251, 117000.
- USGAO, United States Government Accountability Office, 2021. Superfund: EPA should take additional actions to manage risks from climate change effects. GAO-21-555T.
- Uzun, I., 2006. Kinetics of the adsorption of reactive dyes by chitosan. Dyes Pigments 70 (2), 76–83.
- Vanamudan, A., Pamidimukkala, P., 2015. Chitosan, nanoclay and chitosan-nanoclay composite as adsorbents for Rhodamine-6G and the resulting optical properties. Int. J. Biol. Macromol. 74, 127–135.
- Varma, A.J., Deshpande, S.V., Kennedy, J.F., 2004. Metal complexation by chitosan and its derivatives: a review. Carbohydr. Polym. 55 (1), 77–93.
- Wan Ngah, W., Kamari, A., Koay, Y.J., 2004. Equilibrium and kinetics studies of adsorption of copper (II) on chitosan and chitosan/PVA beads. Int. J. Biol. Macromol. 34 (3), 155–161.
- Wan Ngah, W., Ab Ghani, S., Kamari, A., 2005. Adsorption behaviour of Fe (II) and Fe (III) ions in aqueous solution on chitosan and cross-linked chitosan beads. Bioresour. Technol. 96 (4), 443–450.
- Wan Ngah, W., Teong, L.C., Hanafiah, M.M., 2011. Adsorption of dyes and heavy metal ions by chitosan composites: a review. Carbohydr. Polym. 83 (4), 1446–1456.
- Wang, J.W., Kuo, Y.M., 2008. Preparation and adsorption properties of chitosan–poly (acrylic acid) nanoparticles for the removal of nickel ions. J. Appl. Polym. Sci. 107 (4), 2333–2342.
- Wang, L., Wang, A., 2007. Adsorption characteristics of Congo Red onto the chitosan/montmorillonite nanocomposite. J. Hazard Mater. 147 (3), 979–985.
- Wang, S.F., Shen, L., Tong, Y.J., Chen, L., Phang, I.Y., Lim, P.Q., Liu, T.X., 2005. Biopolymer chitosan/montmorillonite nanocomposites: preparation and characterization. Polym. Degrad. Stabil. 90 (1), 123–131.
- Wang, Q.Z., Chen, X.G., Liu, N., Wang, S.X., Liu, C.S., Meng, X.H., Liu, C.G., 2006. Protonation constants of chitosan with different molecular weight and degree of deacetylation. Carbohydr. Polym. 65 (2), 194–201.
- Worch, E., 2012. Adsorption Technology in Water Treatment, vol. 10. de Gruyter, Berlin. Xiang, P., Deng, C., Liu, L., Huang, Y., 2020. Study on the adsorption of methyl red by bentonite/chitosan composites. IOP Conf. Ser. Mater. Sci. Eng. 782 (2), 022079 (IOP Publishing).
- Xie, T., Reddy, K.R., Wang, C., Yargicoglu, E., Spokas, K., 2015. Characteristics and applications of biochar for environmental remediation: a review. Crit. Rev. Environ. Sci. Technol. 45 (9), 939–969.
- Yang, T.C., Zall, R.R., 1984. Absorption of metals by natural polymers generated from seafood processing wastes. Ind. Eng. Chem. Prod. Res. Dev. 23 (1), 168–172.
- Yang, J., Huang, B., Lin, M., 2020. Adsorption of hexavalent chromium from aqueous solution by a chitosan/bentonite composite: isotherm, kinetics, and thermodynamics studies. J. Chem. Eng. Data 65 (5), 2751–2763.
- Yargicoglu, E.N., Sadasivam, B.Y., Reddy, K.R., Spokas, K., 2015. Physical and chemical characterization of waste wood derived biochars. Waste Manag. 36, 256–268.
- Yee, J.J., Arida, C.V.J., Futalan, C.M., de Luna, M.D.G., Wan, M.W., 2019. Treatment of contaminated groundwater via arsenate removal using chitosan-coated bentonite. Molecules 24 (13), 2464.
- Yu, T., Qu, C., Fan, D., Xu, R., 2018. Effects of bentonite activation methods on chitosan loading capacity. Bull. Chem. React. Eng. Catal. 13 (1), 14–23.
- Zhang, L., Hu, P., Wang, J., Huang, R., 2016. Adsorption of Amido Black 10B from aqueous solutions onto Zr (IV) surface-immobilized cross-linked chitosan/bentonite composite. Appl. Surf. Sci. 369, 558–566.
- Zheng, L., Gao, Y., Du, J., Zhang, W., Huang, Y., Wang, L., et al., 2020. A novel, recyclable magnetic biochar modified by chitosan–EDTA for the effective removal of Pb (II) from aqueous solution. RSC Adv. 10 (66), 40196–40205.
- Zhou, Y., Gao, B., Zimmerman, A.R., Fang, J., Sun, Y., Cao, X., 2013. Sorption of heavy metals on chitosan-modified biochars and its biological effects. Chem. Eng. J. 231, 512–518.